



US012599332B2

(12) **United States Patent**  
**Dagum et al.**

(10) **Patent No.:** **US 12,599,332 B2**  
(45) **Date of Patent:** **\*Apr. 14, 2026**

(54) **NON-INVASIVE ASSESSMENT OF GLYMPHATIC FLOW AND NEURODEGENERATION FROM A WEARABLE DEVICE**

(71) Applicant: **Applied Cognition, Inc.**, Los Altos Hills, CA (US)

(72) Inventors: **Paul Dagum**, Los Altos Hills, CA (US); **Gregory T. A. Kovacs**, Palo Alto, CA (US); **Laurent B. Giovangrandi**, Palo Alto, CA (US); **Carl J. Weber**, Portola Valley, CA (US); **Joerg C. Student**, San Francisco, CA (US); **Nathan Whipple**, San Francisco, CA (US); **Jonathan I. Kaplan**, Palo Alto, CA (US)

(73) Assignee: **Applied Cognition, Inc.**, Redwood City, CA (US)

(\* ) Notice: Subject to any disclaimer, the term of this patent is extended or adjusted under 35 U.S.C. 154(b) by 0 days.

This patent is subject to a terminal disclaimer.

(21) Appl. No.: **18/636,234**

(22) Filed: **Apr. 15, 2024**

(65) **Prior Publication Data**  
US 2024/0268748 A1 Aug. 15, 2024

**Related U.S. Application Data**

(63) Continuation of application No. 18/451,100, filed on Aug. 17, 2023, now abandoned, which is a (Continued)

(51) **Int. Cl.**  
**A61B 5/00** (2006.01)  
**A61B 5/0205** (2006.01)  
**A61B 5/372** (2021.01)

(52) **U.S. Cl.**  
CPC ..... **A61B 5/4088** (2013.01); **A61B 5/0006** (2013.01); **A61B 5/0205** (2013.01); (Continued)

(58) **Field of Classification Search**  
CPC ... **A61B 5/4088**; **A61B 5/0006**; **A61B 5/0205**; **A61B 5/372**; **A61B 5/418**; **A61B 5/6817**; (Continued)

(56) **References Cited**

**U.S. PATENT DOCUMENTS**

4,601,294 A \* 7/1986 Danby ..... A61B 5/12 600/379  
4,706,682 A \* 11/1987 Stypulkowski ..... A61B 5/283 607/116

(Continued)

**FOREIGN PATENT DOCUMENTS**

SE 543899 C2 9/2021  
WO 2019169142 9/2019

(Continued)

**OTHER PUBLICATIONS**

Goverdovsky et al, "In-Ear EEG From Viscoelastic Generic Earpieces: Robust and Unobtrusive 24/7 Monitoring", IEEE Sensors Journal, Jan. 1, 2016, pp. 271-277, vol. 16, No. 1.

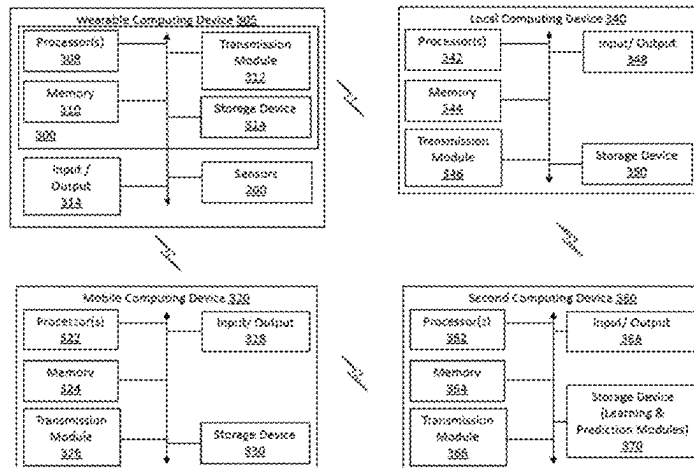
(Continued)

*Primary Examiner* — Rene T Towa  
(74) *Attorney, Agent, or Firm* — King & Spalding LLP

(57) **ABSTRACT**

A computer-implemented method and system includes accessing neurophysiological and neurovascular data recorded during sleep. A function mapping is executed from said neurophysiological and neurovascular data to a target that is one of a glymphatic flow marker, a molecular analysis marker of neurodegeneration, or a neuroimaging marker of neurodegeneration. A target prediction model is output based on the function mapping. The target prediction model

(Continued)



can receive new neurophysiological and neurovascular data and output a predicted marker of neurodegeneration.

**30 Claims, 28 Drawing Sheets**

**Related U.S. Application Data**

continuation of application No. 17/937,952, filed on Oct. 4, 2022, now Pat. No. 11,759,142, which is a continuation of application No. 17/713,329, filed on Apr. 5, 2022, now Pat. No. 11,478,184.

(60) Provisional application No. 63/244,080, filed on Sep. 14, 2021.

(52) **U.S. Cl.**  
CPC ..... *A61B 5/372* (2021.01); *A61B 5/418* (2013.01); *A61B 5/6817* (2013.01); *A61B 5/7275* (2013.01); *A61B 2562/166* (2013.01)

(58) **Field of Classification Search**  
CPC ..... A61B 5/7275; A61B 2562/166; A61B 5/4806; A61B 5/4064; G01R 33/5601; G01R 33/56341  
See application file for complete search history.

(56) **References Cited**

U.S. PATENT DOCUMENTS

6,511,437	B1	1/2003	Nakamura	
6,640,121	B1	10/2003	Telischi et al.	
7,209,775	B2	4/2007	Bae et al.	
8,277,385	B2	10/2012	Berka	
8,884,767	B2	11/2014	Kidmose	
8,926,542	B2	1/2015	Gerber	
9,025,800	B2	5/2015	Kidmose et al.	
9,210,517	B2	12/2015	Pontoppidan et al.	
9,307,918	B2	4/2016	Kinrot	
9,408,552	B2	8/2016	Kidmose et al.	
9,918,650	B2	3/2018	Kilsgaard et al.	
9,949,045	B2	4/2018	Kure et al.	
10,052,065	B2	8/2018	Boesen	
10,194,228	B2	1/2019	Hirsch	
10,275,027	B2	4/2019	Segal	
10,433,788	B2	10/2019	Boesen	
10,542,904	B2	1/2020	Durand	
10,575,777	B2	3/2020	Ayers et al.	
10,606,354	B2	3/2020	Segal	
10,617,297	B2	4/2020	Turner	
10,728,642	B2	7/2020	Solum et al.	
10,743,121	B2	8/2020	Pontoppidan et al.	
10,765,337	B2	9/2020	Andersen	
10,798,487	B2	10/2020	Hviid	
10,835,145	B1	11/2020	Prevoir et al.	
10,841,682	B2	11/2020	Masaki et al.	
10,856,063	B1	12/2020	Hviid	
10,856,071	B2	12/2020	Verdooner et al.	
11,298,542	B2	4/2022	Aur	
11,759,142	B2*	9/2023	Dagum ..... G16H 50/20 600/544	
12,133,738	B2	11/2024	Dagum	
2005/0059870	A1*	3/2005	Aceti ..... A61B 7/003 600/595	
2007/0112277	A1	5/2007	Fischer et al.	
2007/0287899	A1*	12/2007	Poupko ..... A61B 5/053 600/383	
2008/0275352	A1	11/2008	Shapira	
2009/0264776	A1	10/2009	Vardy	
2010/0130884	A1*	5/2010	Linninger ..... A61B 5/053 600/561	
2011/0196245	A1	8/2011	Poupko	
2011/0251503	A1	10/2011	Ben-Ari	

2012/0165695	A1	6/2012	Kidmose et al.	
2012/0302858	A1	11/2012	Kidmose et al.	
2013/0085356	A1	4/2013	Schlottau	
2014/0018649	A1	1/2014	Jespersen	
2015/0011898	A1*	1/2015	Romesburg ..... A61B 5/6801 600/479	
2016/0000945	A1*	1/2016	Nedergaard ..... A61P 25/16 604/9	
2016/0022195	A1	1/2016	Vardy	
2016/0310028	A1	10/2016	Kidmose et al.	
2016/0317085	A1	11/2016	Razavi	
2017/0224949	A1	8/2017	Acton	
2017/0251950	A1	9/2017	Piron et al.	
2017/0311870	A1	11/2017	Bardakjian et al.	
2017/0311881	A1	11/2017	Jensen et al.	
2018/0014741	A1	1/2018	Chou	
2018/0055398	A1	3/2018	Westermann et al.	
2018/0177421	A1	6/2018	Kilsgaard et al.	
2018/0220903	A1	8/2018	LeBoeuf et al.	
2018/0228381	A1	8/2018	LeBoeuf et al.	
2018/0235540	A1	8/2018	Kirszenblat et al.	
2018/0271428	A1	9/2018	Takagi et al.	
2018/0277238	A1	9/2018	Boesen	
2018/0277245	A1	9/2018	Boesen	
2018/0353095	A1	12/2018	Boesen	
2018/0368718	A1	12/2018	Koziol	
2019/0174238	A1	6/2019	Lunner et al.	
2019/0201684	A1*	7/2019	Williams ..... A61N 1/36132	
2019/0209038	A1	7/2019	Saab et al.	
2019/0223747	A1	7/2019	Chou	
2019/0253793	A1	8/2019	Pedersen et al.	
2019/0269336	A1	9/2019	Perkins et al.	
2019/0282119	A1	9/2019	Andersen et al.	
2019/0380597	A1	12/2019	Howard	
2019/0380648	A1	12/2019	Kirszenblat	
2020/0085331	A1	3/2020	Chou	
2020/0225750	A1	7/2020	Segal	
2020/0268265	A1	8/2020	Walsh et al.	
2020/0288253	A1	9/2020	De Haan et al.	
2020/0306493	A1	10/2020	Lee	
2021/0241909	A1	8/2021	Bulut	
2021/0275097	A1	9/2021	Pushpala	
2021/0282698	A1	9/2021	Garcia Molina	
2022/0000421	A1	1/2022	Ippolito	

FOREIGN PATENT DOCUMENTS

WO	2020035852	2/2020
WO	2020061209	3/2020
WO	2020127940	6/2020
WO	2020210813	10/2020
WO	2022180306	9/2022

OTHER PUBLICATIONS

Goverdovsky et al. "Hearables: Multimodal physiological in-ear sensing", Scientific Reports, Jul. 31, 2017, pp. 1-10, 7: 6948 | DOI:10.1038/s41598-017-06925-2.

R. Kusche et al., "An in-ear pulse wave velocity measurement system using heart sounds as time reference", Current Directions in Biomedical Engineering 2015; 1:366-370, De Gruyter.

Kwon, Shinjae, Hojoong Kim, and Woon-Hong Yeo; "Recent Advances in Wearable Sensors and Portable Electronics for Sleep Monitoring"; iScience 24.5 (2021): 102461 (Year: 2021).

Hablitz, Lauren M., et al.; "Increased Glymphatic Influx Is Correlated With Hight EEG Delta Power and Low Heart Rate in Mice Under Anesthesia"; Science Advances 5.2 (2019); eaav5447; (Year: 2019).

Tanabe, Sean, et al. "Cohort Study of Electroencephalography Markers of Amyloid-Tau-Neurodegeneration Pathology."; Brain Communications 2.2 (2020): fcaa099. (Year:2020).

International Search Report and Written Opinion issued in PCT Application No. PCT/US2022/023409, mailed Jul. 25, 2022, 9 pages, Korean Intellectual Property Office.

Meghdadi, Amir H., et al. "Transcranial Impedance Changes During Sleep: A Rheoencephalography Study," IEEE Journal of Transla-

(56)

**References Cited**

OTHER PUBLICATIONS

tional Engineering In Health and Medicine 7 (2019): 1-7 (Year: 2019).

Guermendi, Marco, et al. "Active electrode IC for EEG and electrical impedance tomography with continuous monitoring of contact impedance." IEEE transactions on biomedical circuits and systems 9.1 (2014): 21-33 (Year: 2014).

International Search Report and Written Opinion for PCT Patent Application No. PCT/US2023/077566 dated Feb. 19, 2024.

International Search Report and Written Opinion for PCT Patent Application No. PCT/US2023/077562 dated Feb. 19, 2024.

Moskalenko, Yu; Multifrequency REG: Fundamental Background, Information Meaning and Ways of Data Analysis and Automation; Am. J. Biomedical Eng'g; 2012; 2(4): 163-174.

Taoka, Taoshiaki; Neurofluid Dynamics and the Glymphatic System: A Neuroimaging Perspective; Korean J. of Radiology; 2020; 21(11):1199-1209.

European Patent Office Search Report for EP App. No. 22870452.4, dated Jun. 10, 2025, 13 pages.

Wendt, Karen; et al.; Physiology Informed Neuromodulation; J. Neurological Science; Mar. 15, 2022; 434:120121.

Dagum, Paul; et al.; "The Use Of Continuous Brain Parenchymal Impedance Dispersion To Measure Glymphatic Function In Humans"; MedRxiv; Jan. 9, 2024; <https://www.medrxiv.org/>.

\* cited by examiner

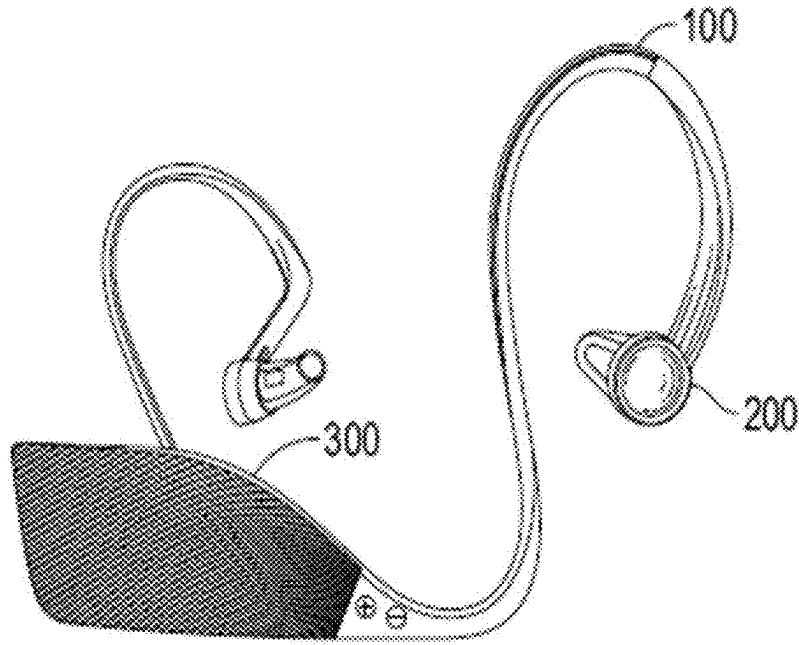


FIG. 1A

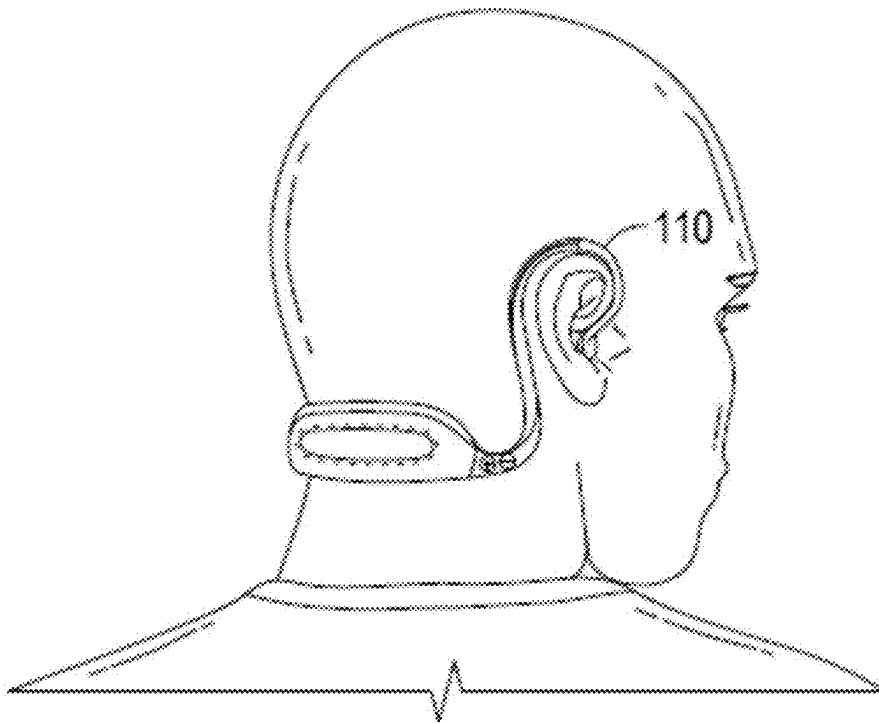


FIG. 1B

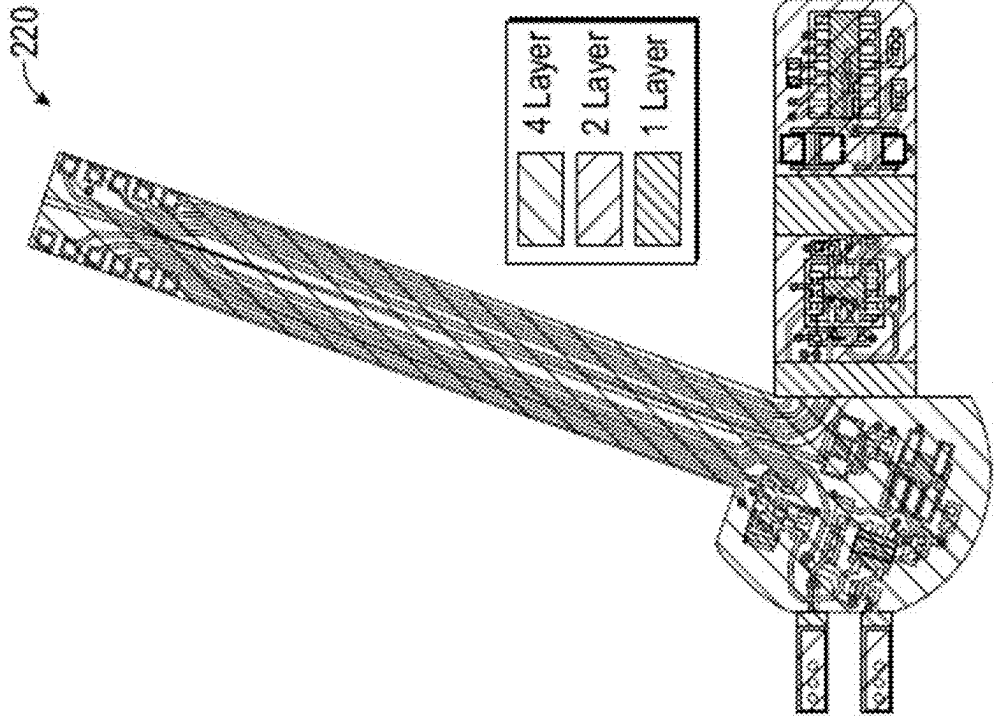


FIG. 2A

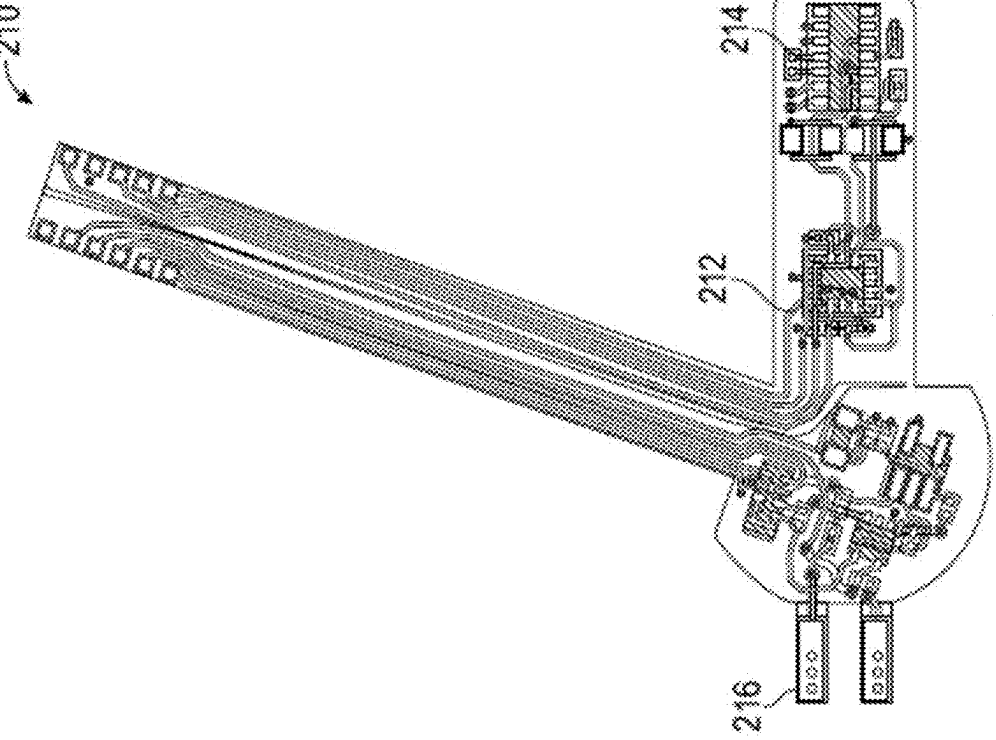


FIG. 2B

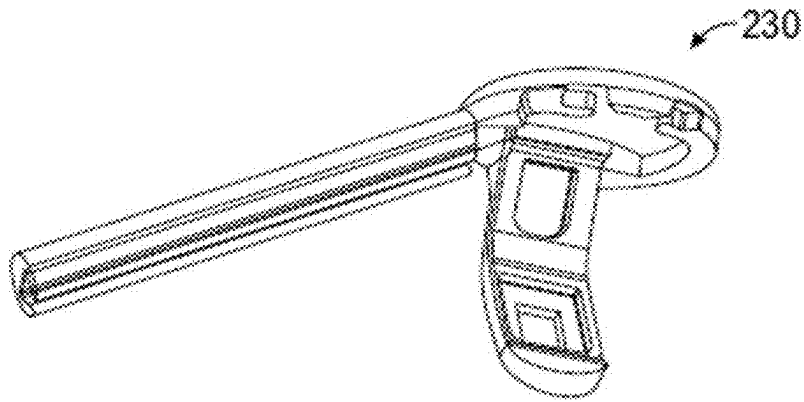


FIG. 2C

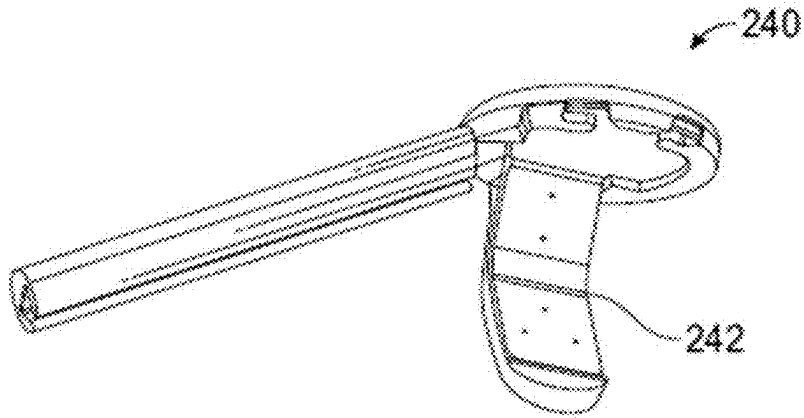


FIG. 2D

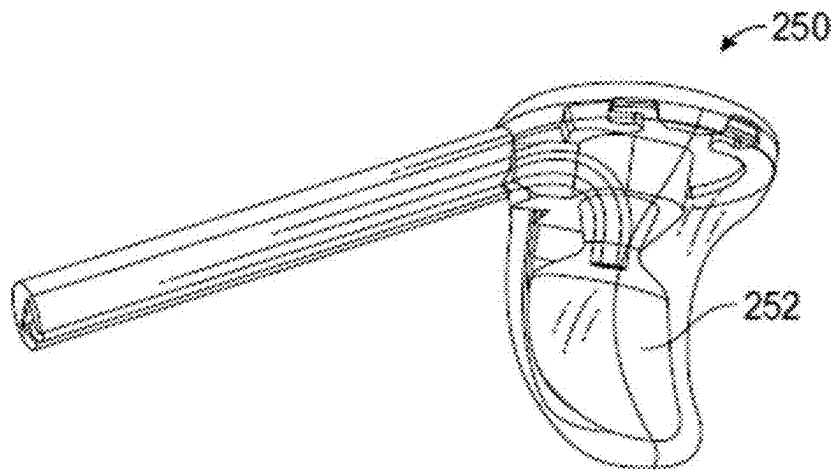


FIG. 2E

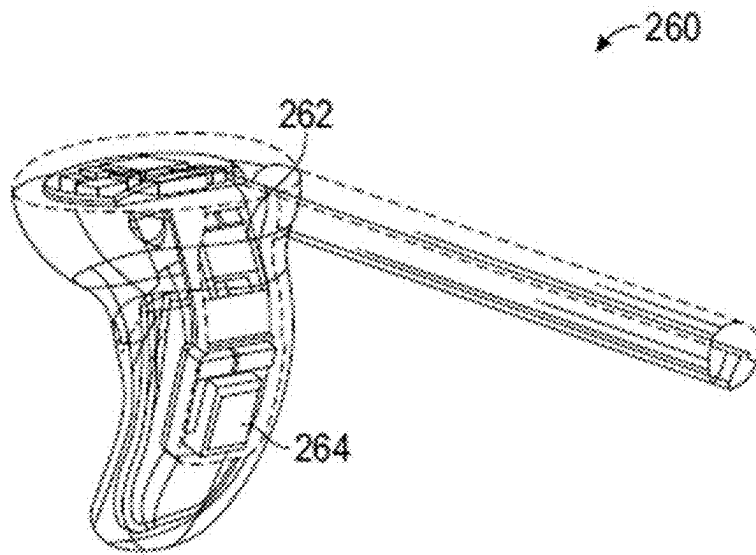


FIG. 2F

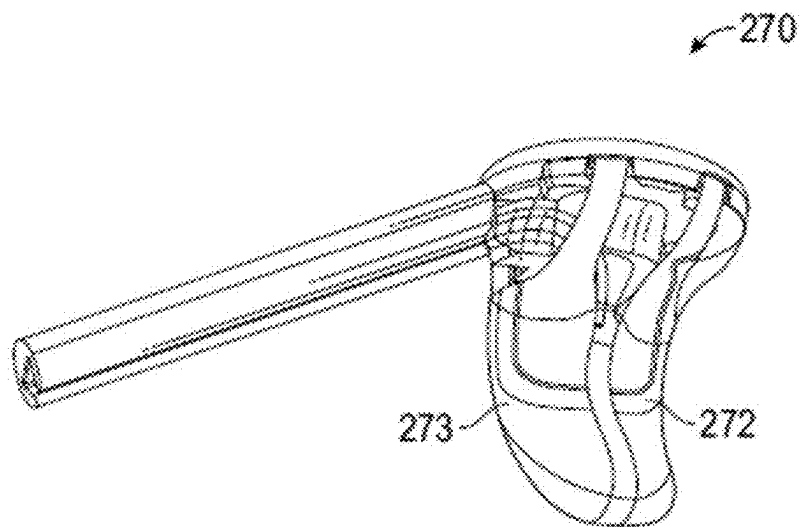


FIG. 2G

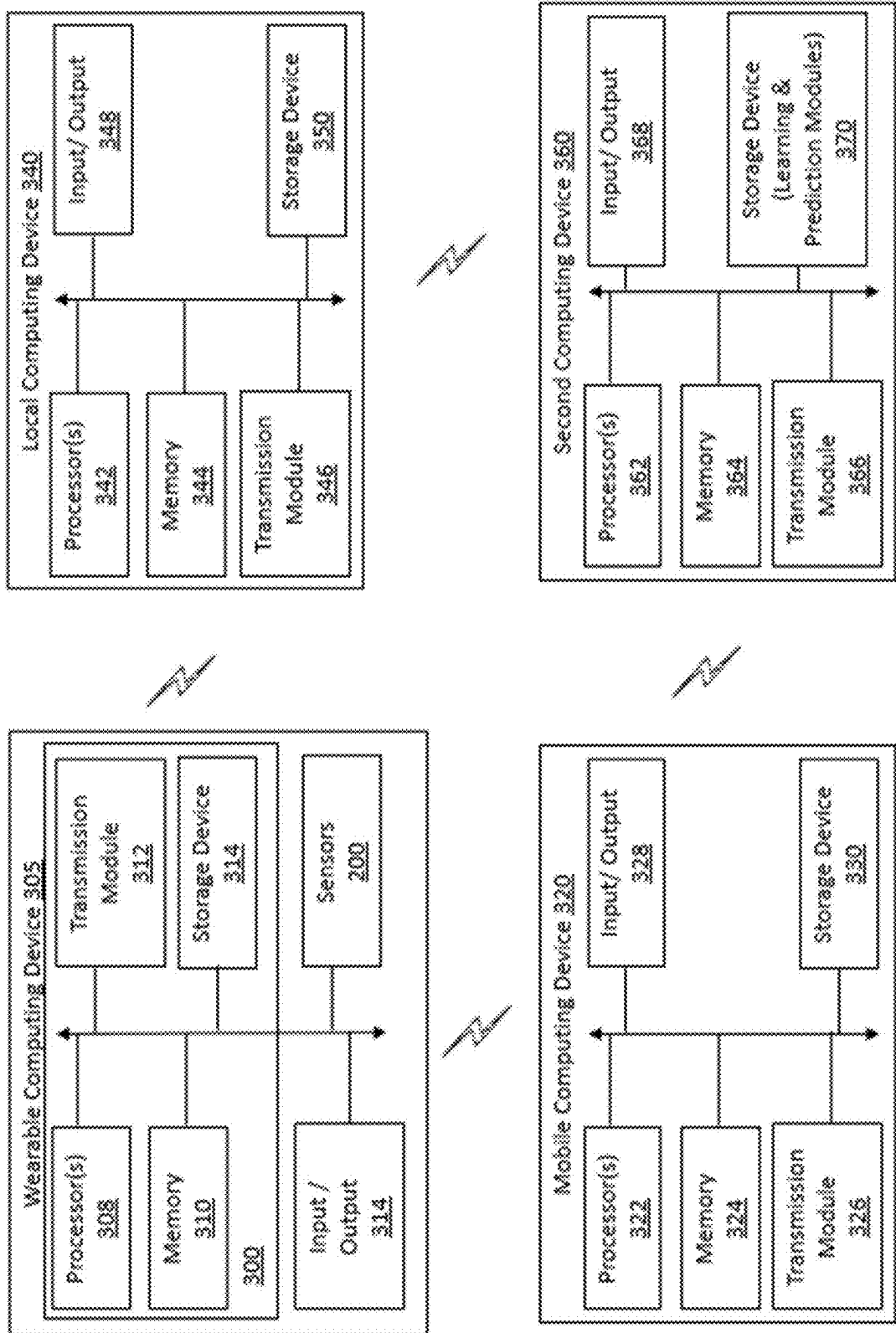


FIG. 3

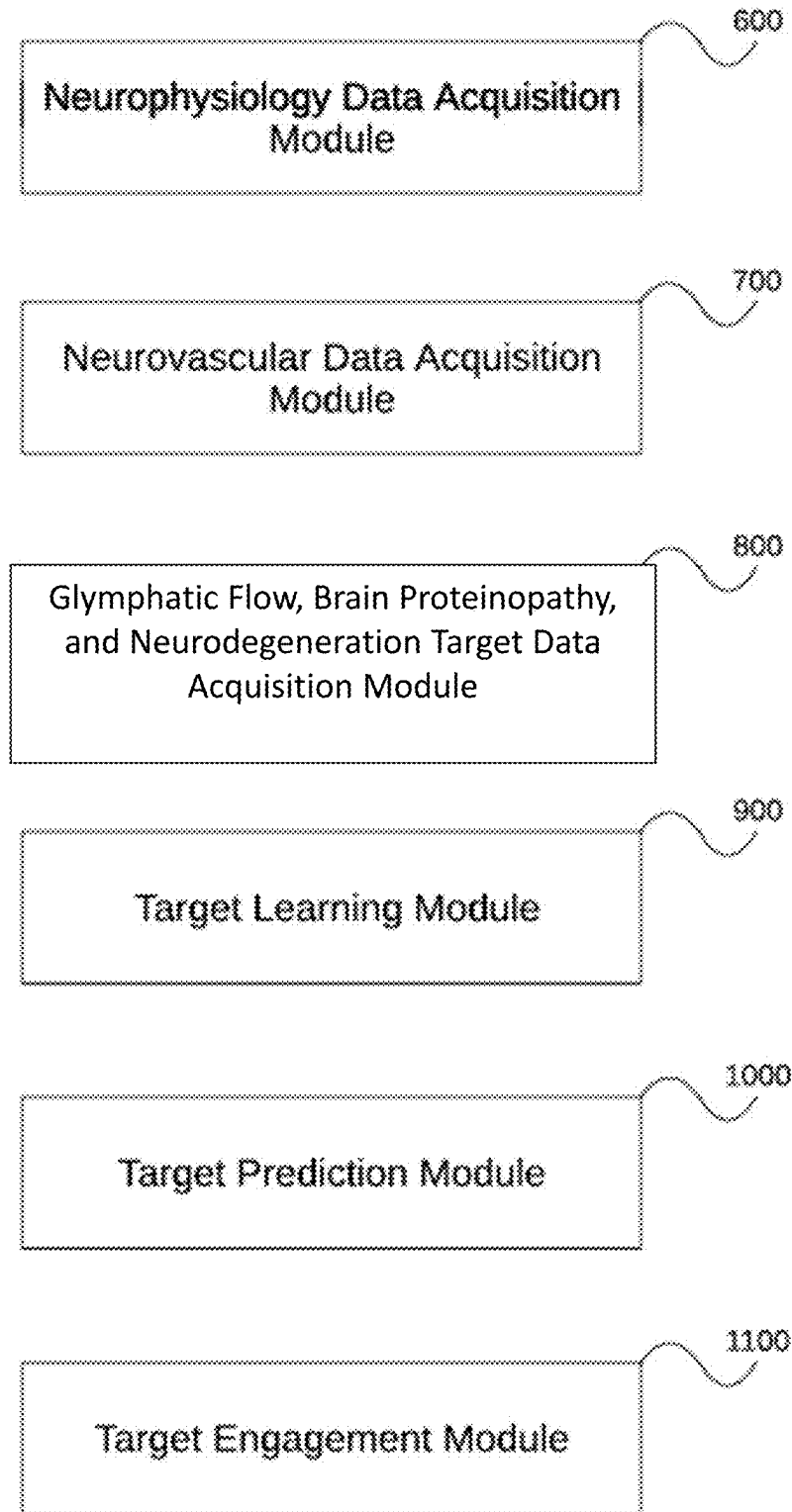


FIG. 4

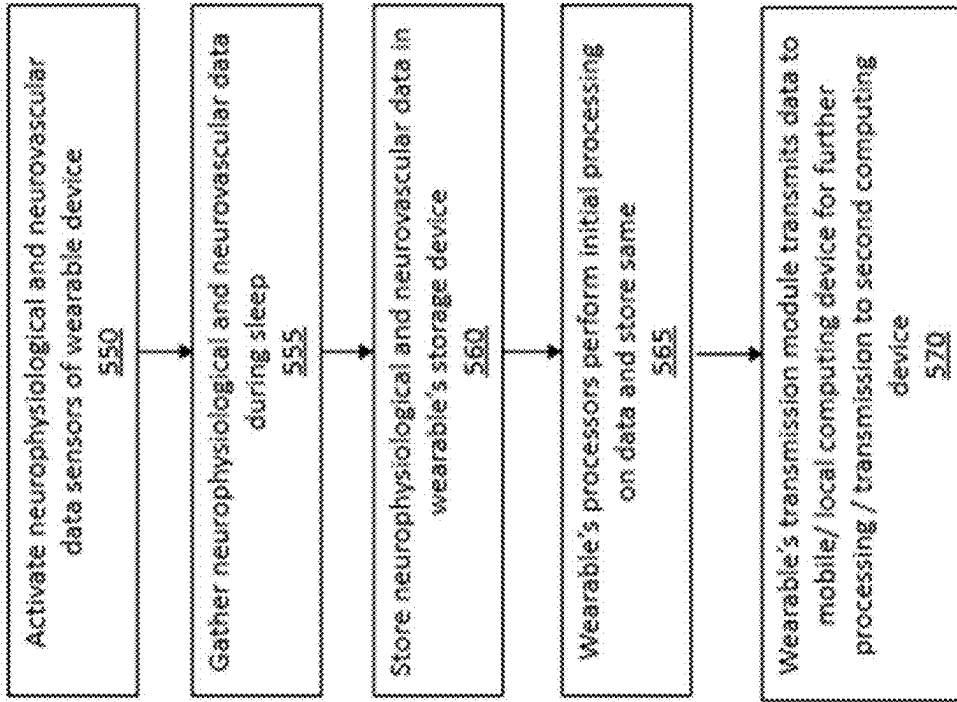


FIG. 5 B

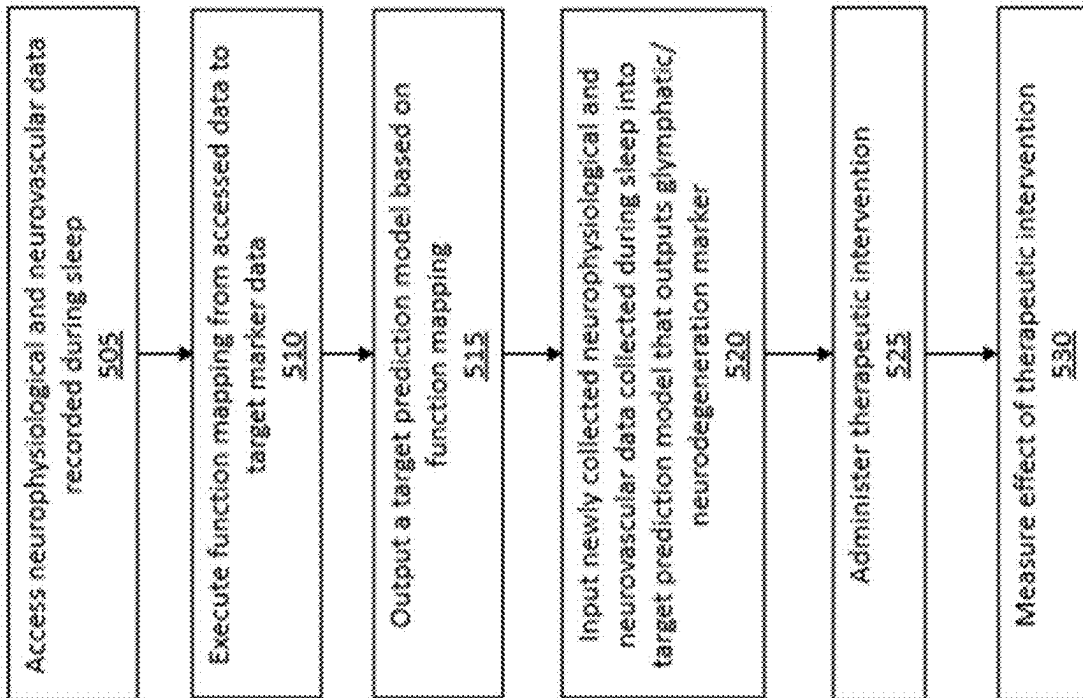


FIG. 5 A

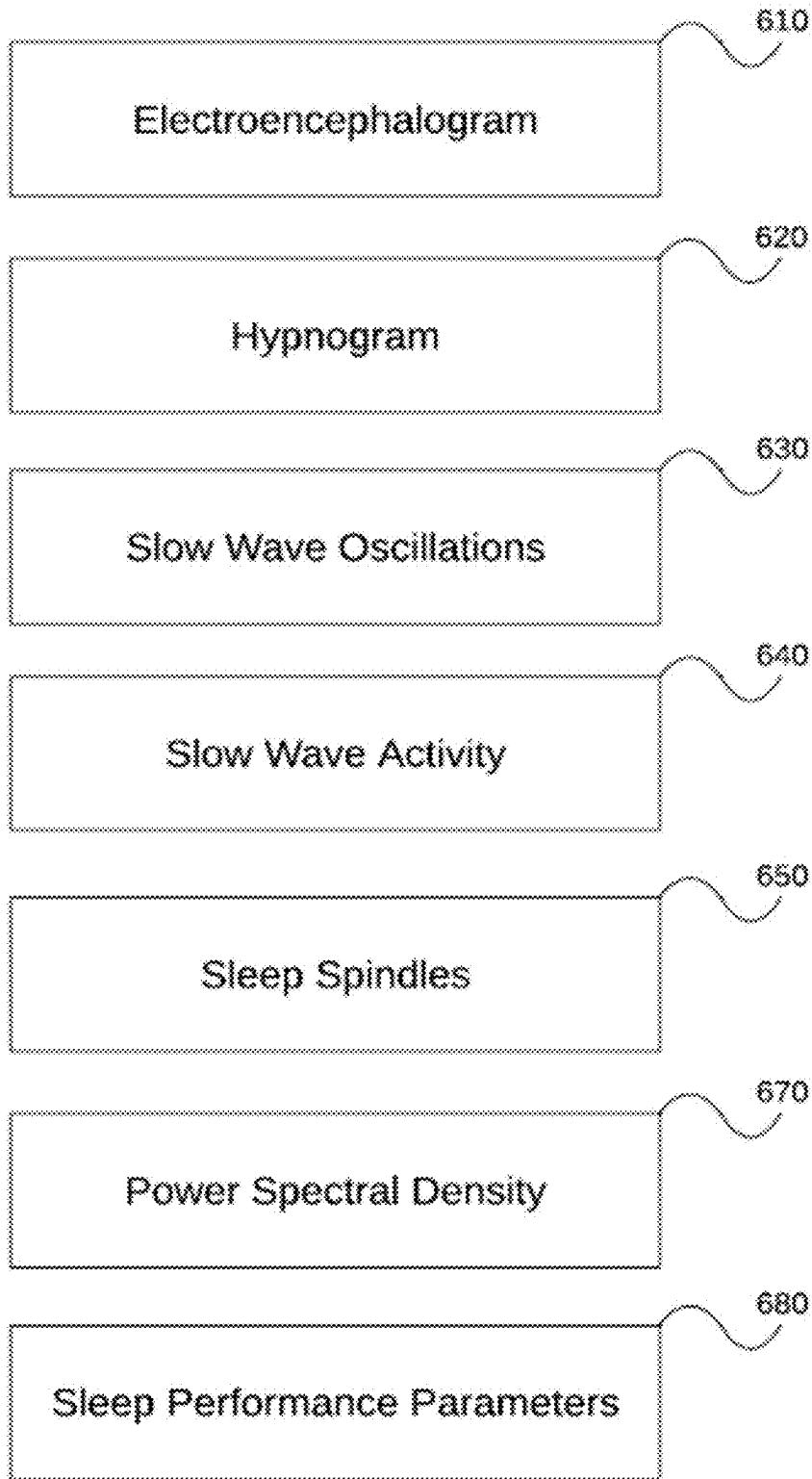
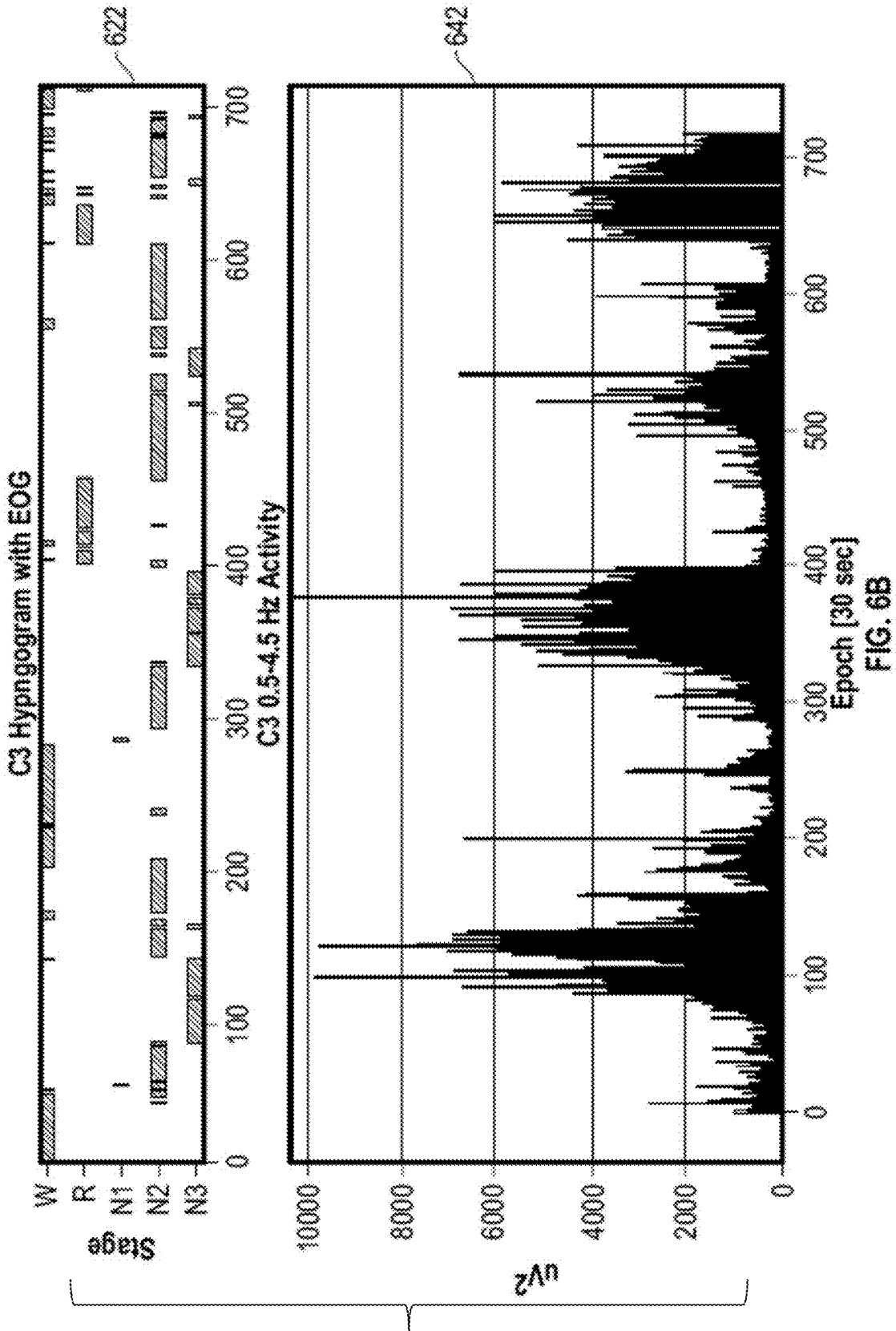


FIG. 6A



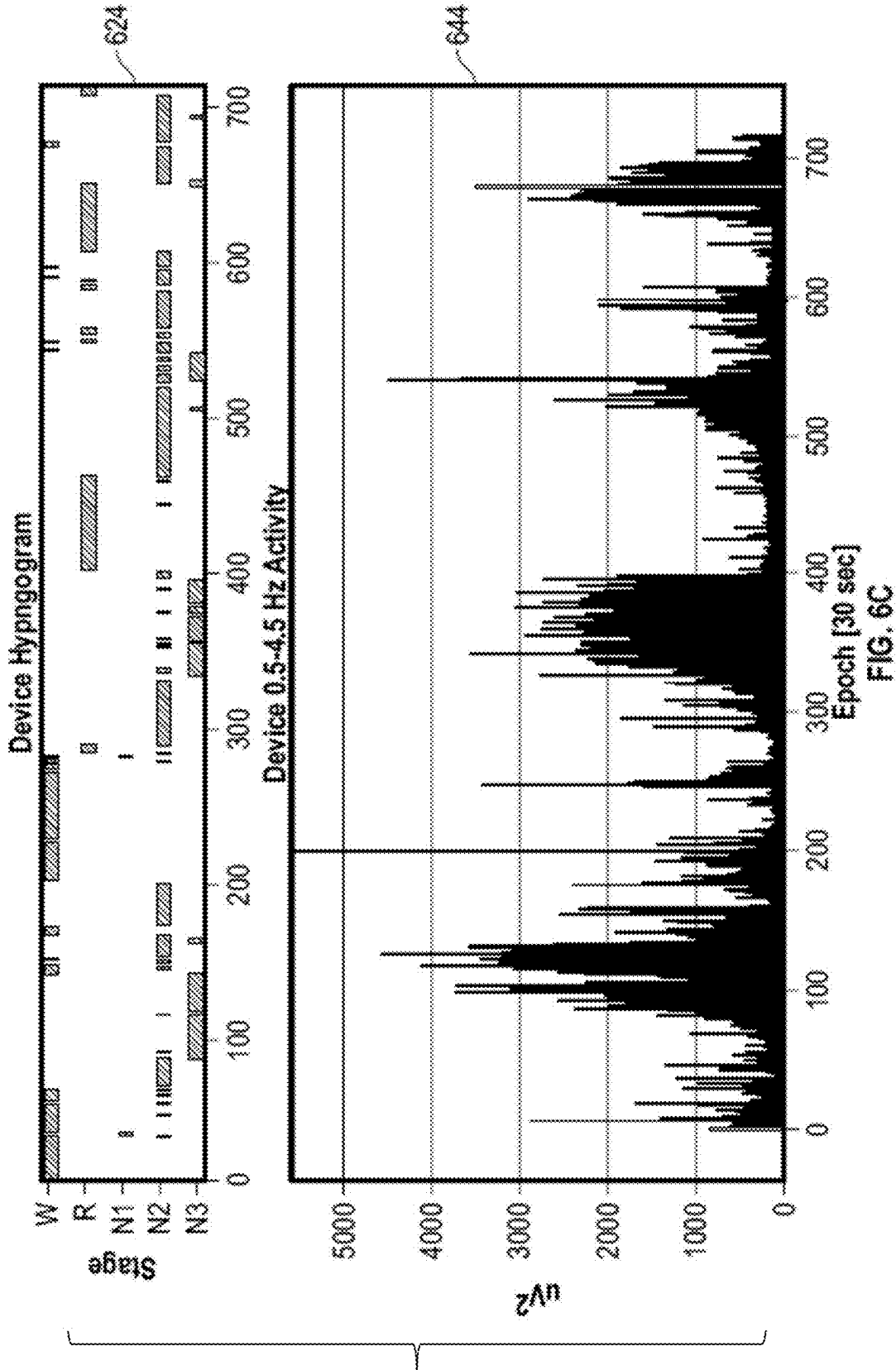
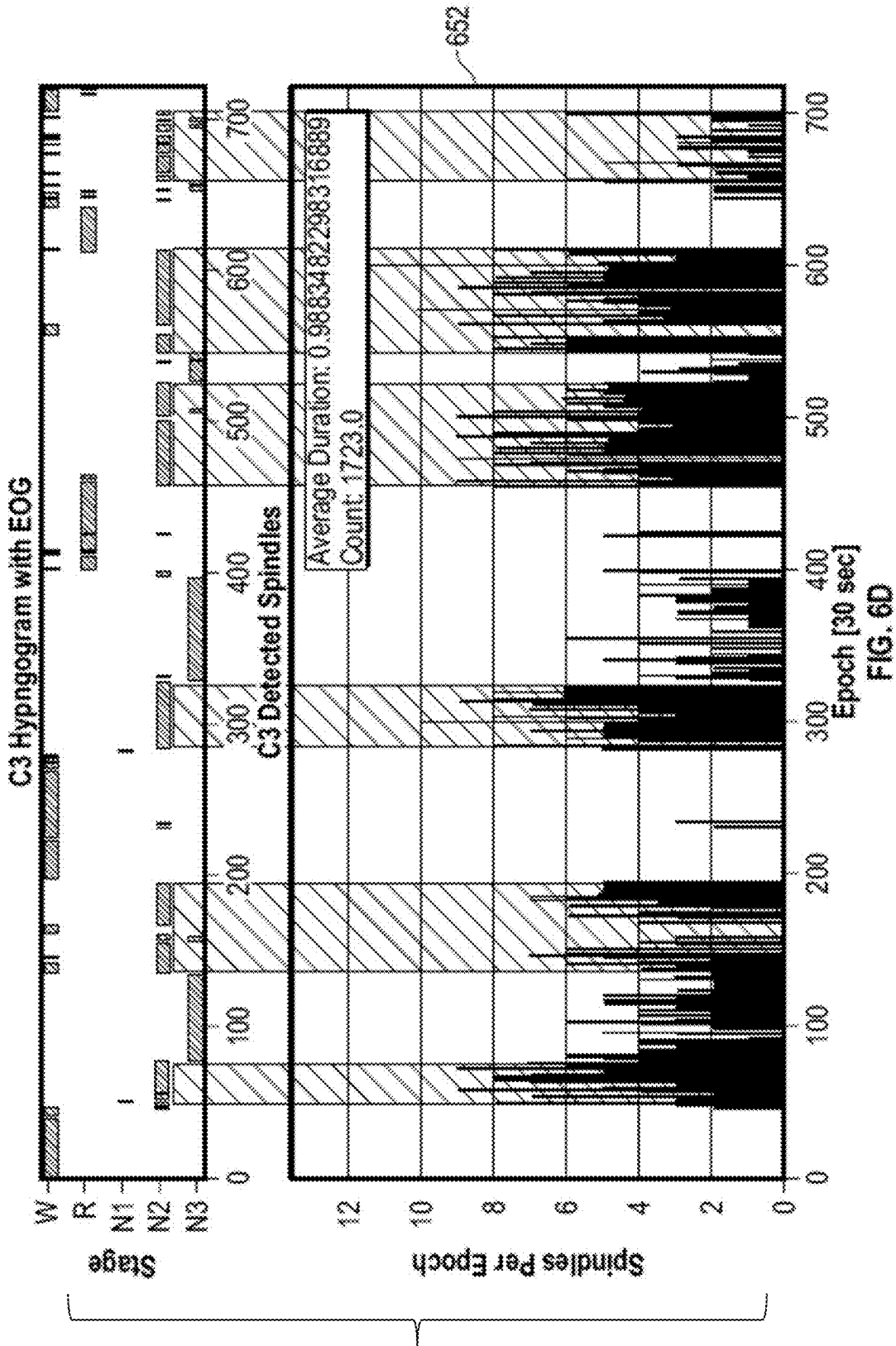


FIG. 6C



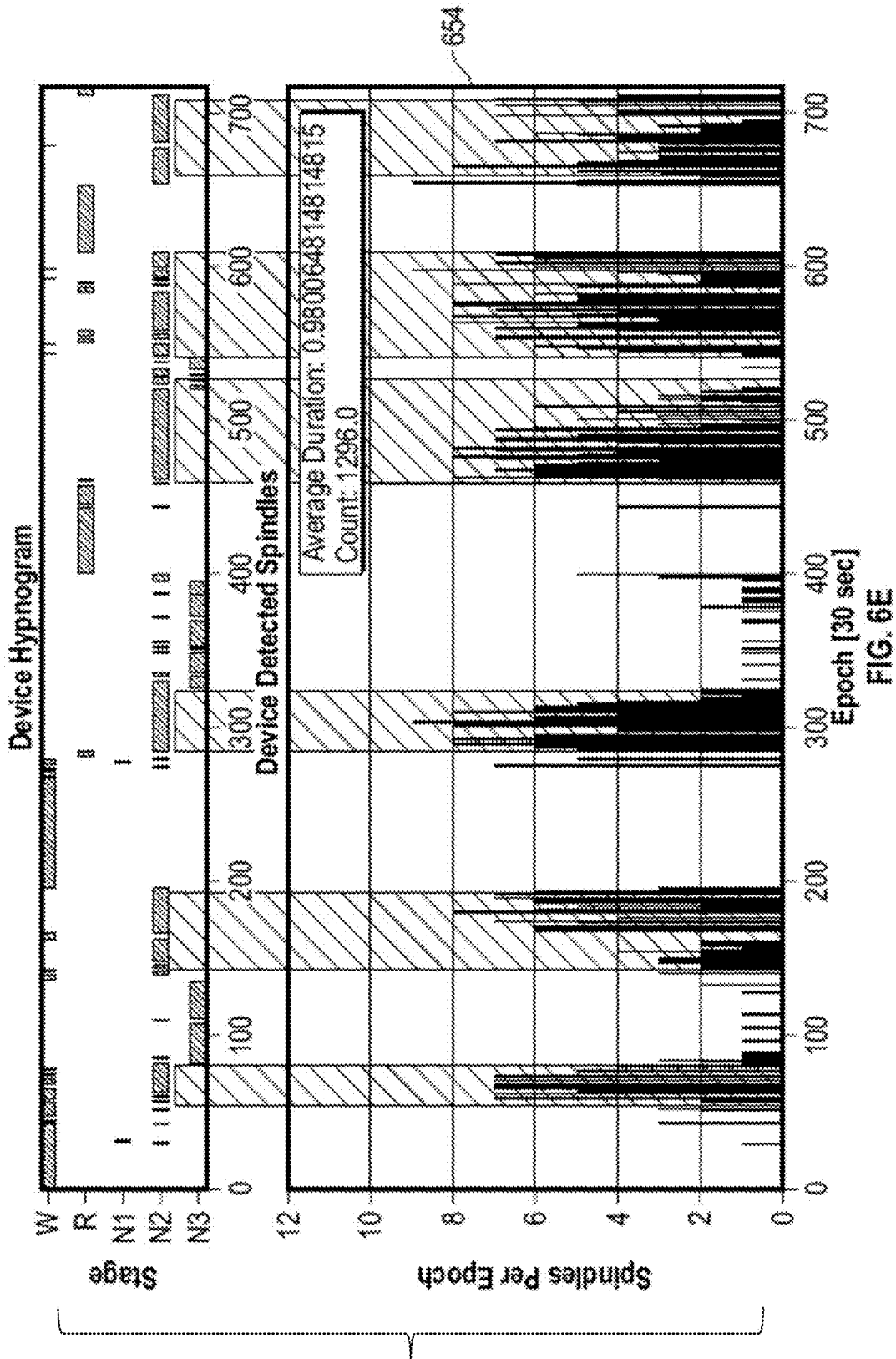


FIG. 6E

682

MEASURE	Value (%)
Sensitivity for Wake	69
Sensitivity for Light Sleep (N1 or N2)	80
Sensitivity for SWS (N3)	88
Sensitivity for REM	99
Overall agreement	81

684

MEASURE	EEG	Device
Total Sleep Time (min)	270	282
Sleep Onset Latency (min)	23	23
Wake After Sleep Onset (min)	65	62
Sleep Efficiency (%)	75	79
Number of Awakenings	22	18

FIG. 6F

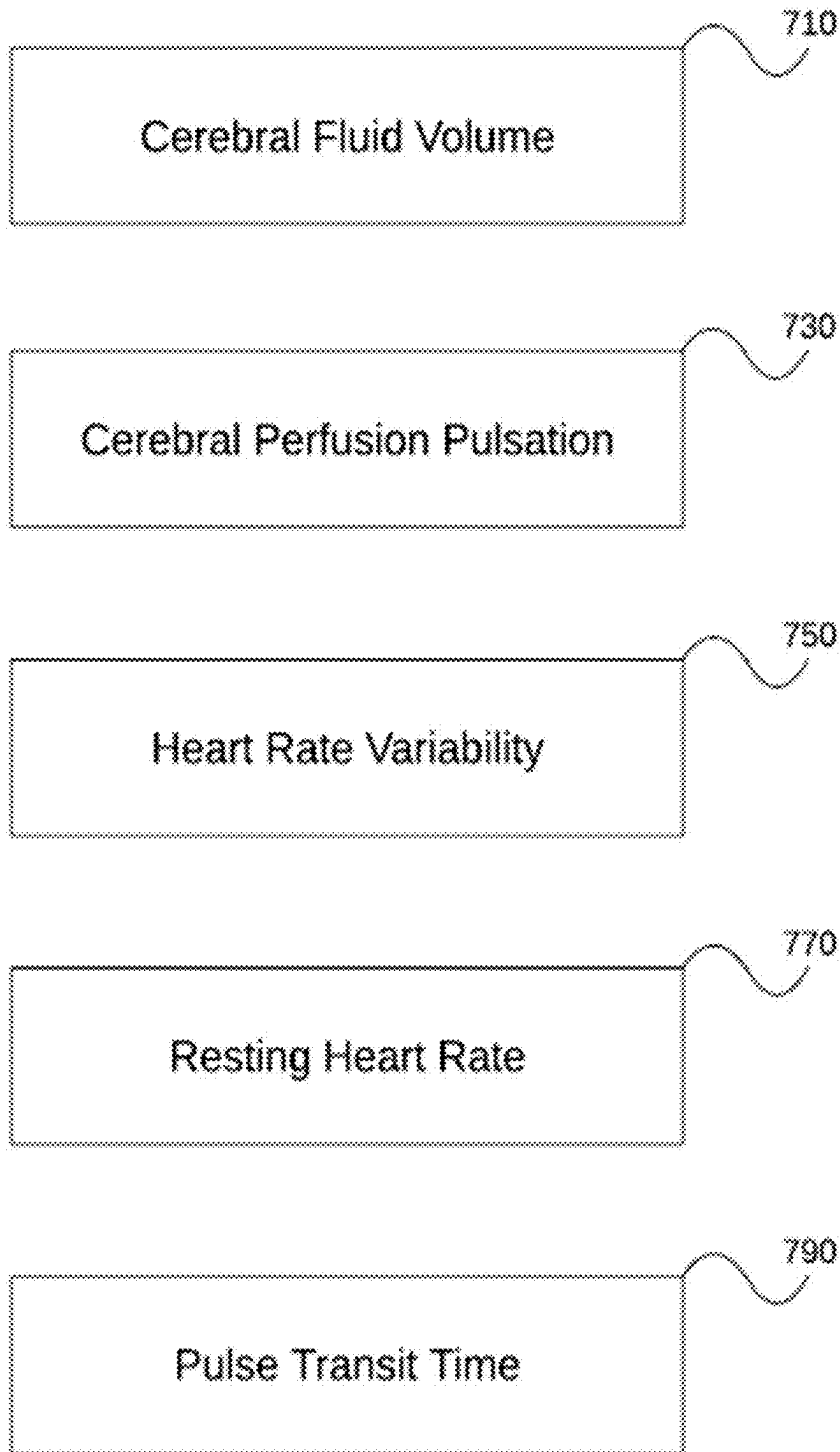


FIG. 7A

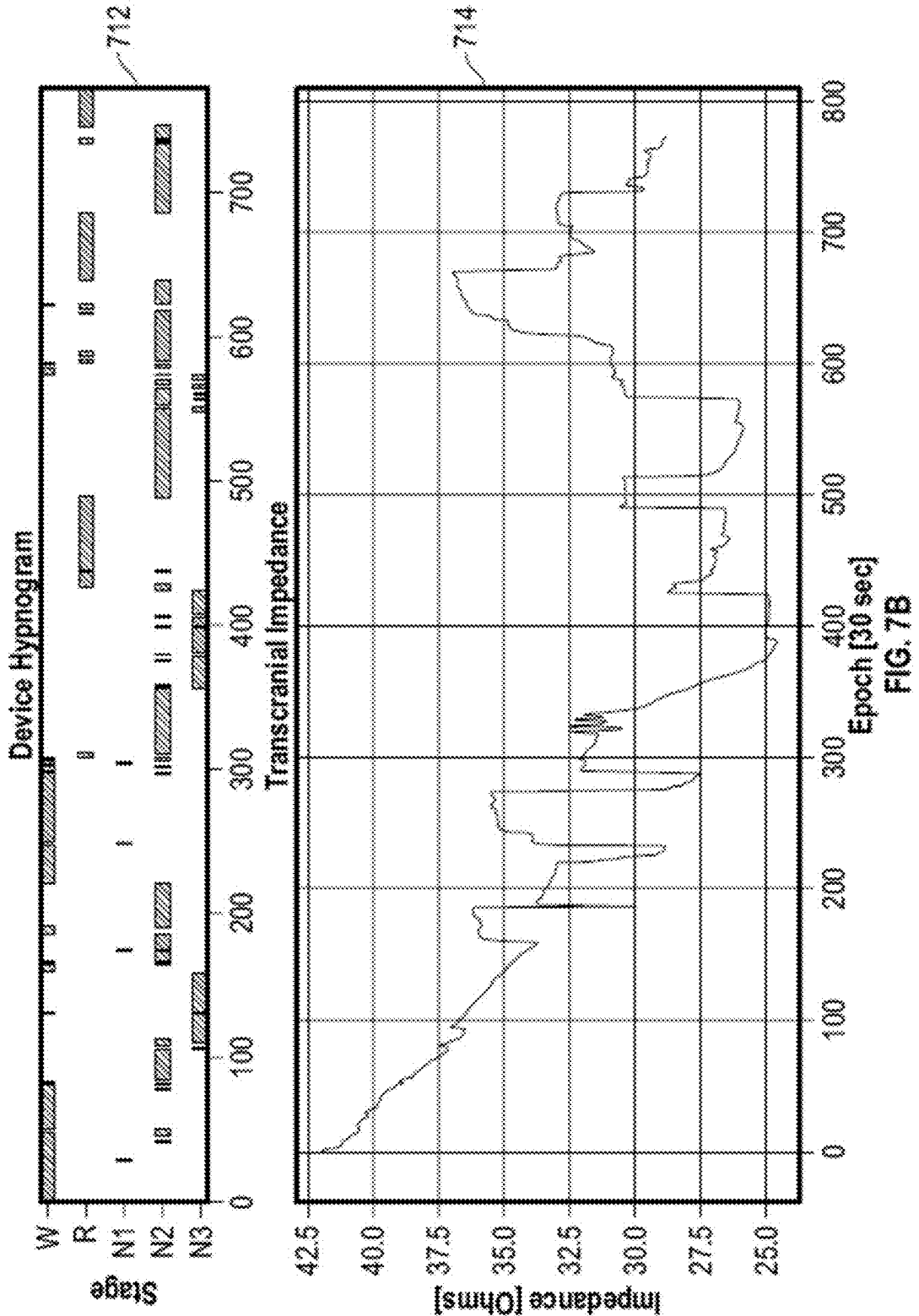


FIG. 7B

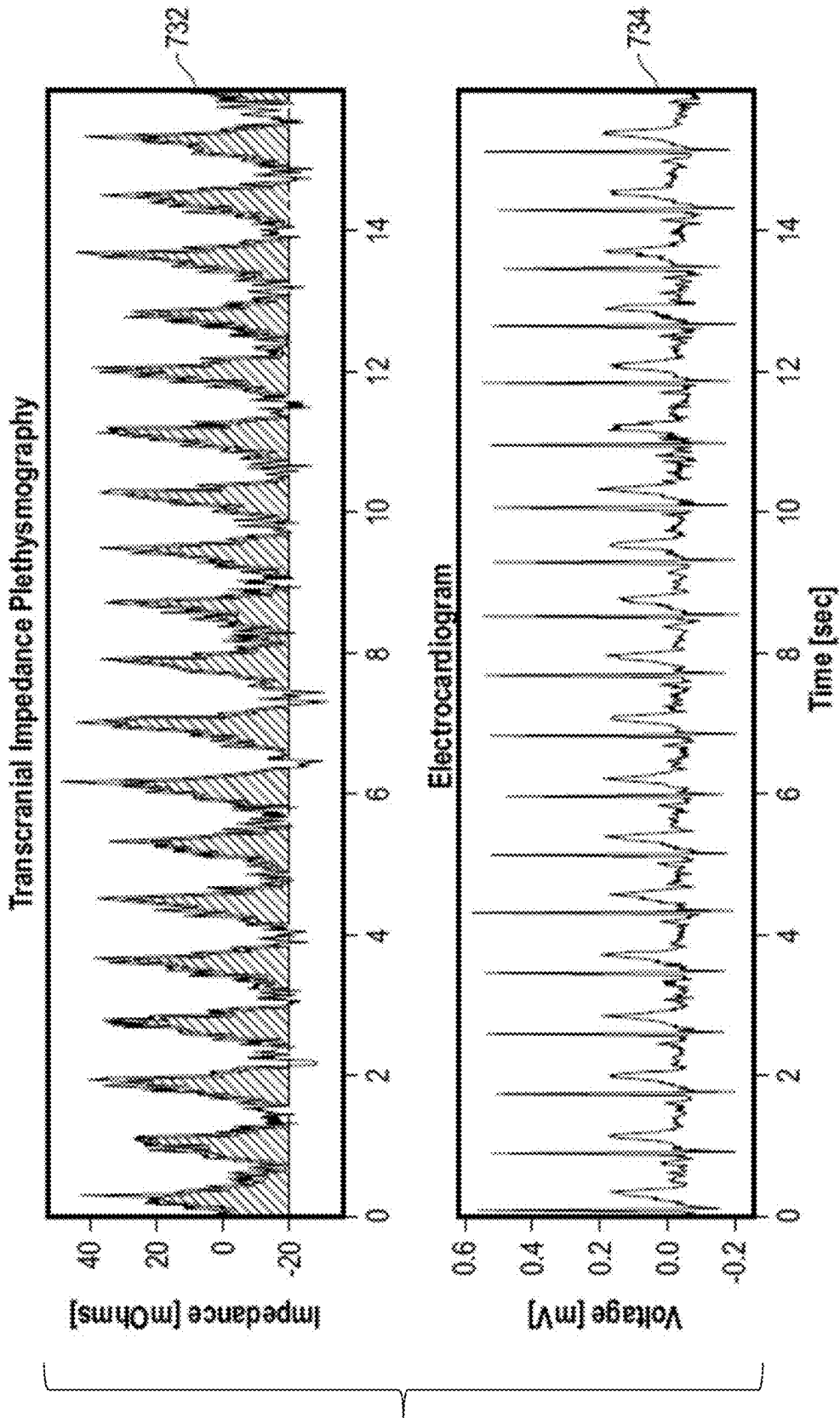


FIG. 7B cont.

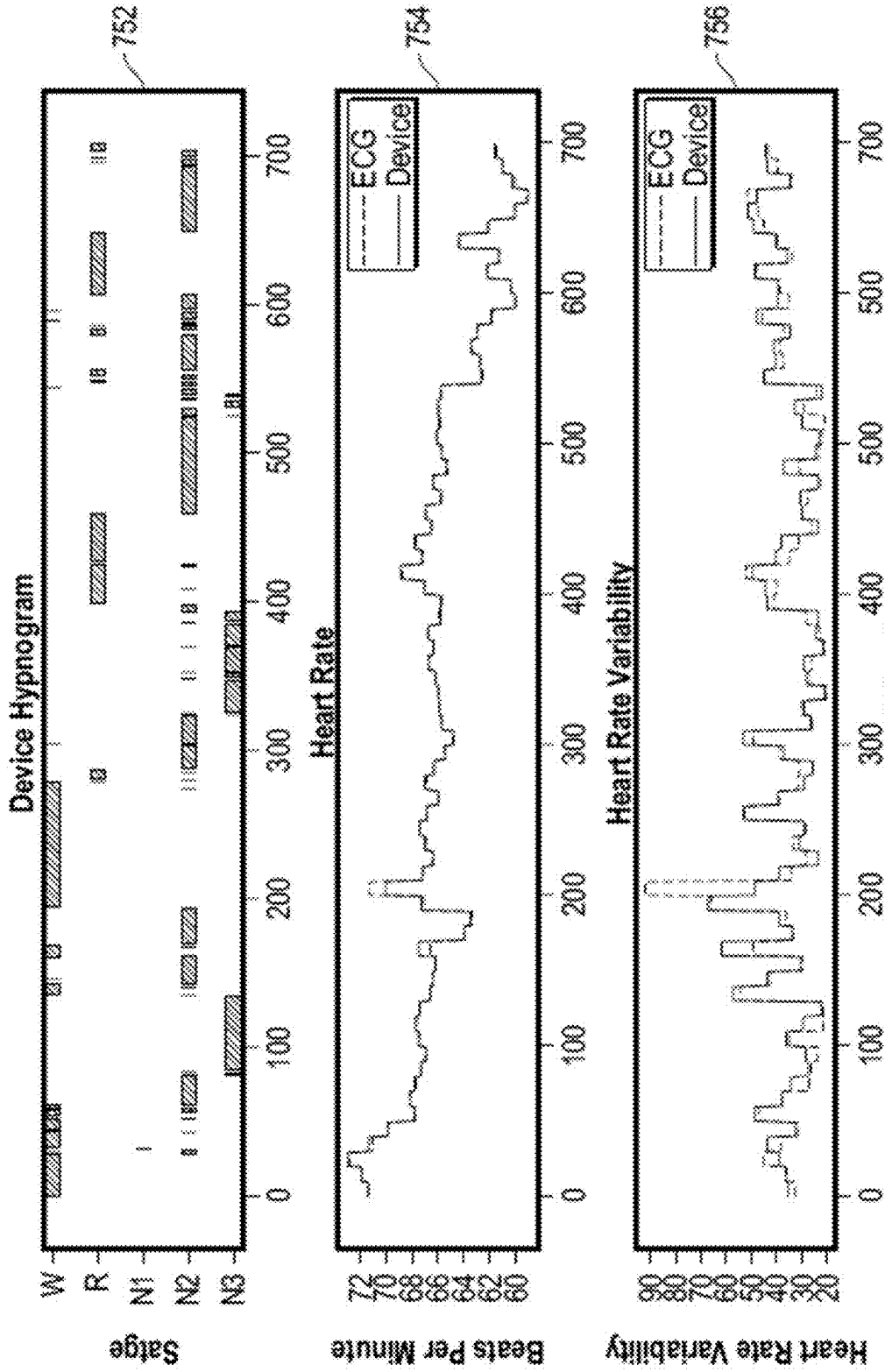


FIG. 7C

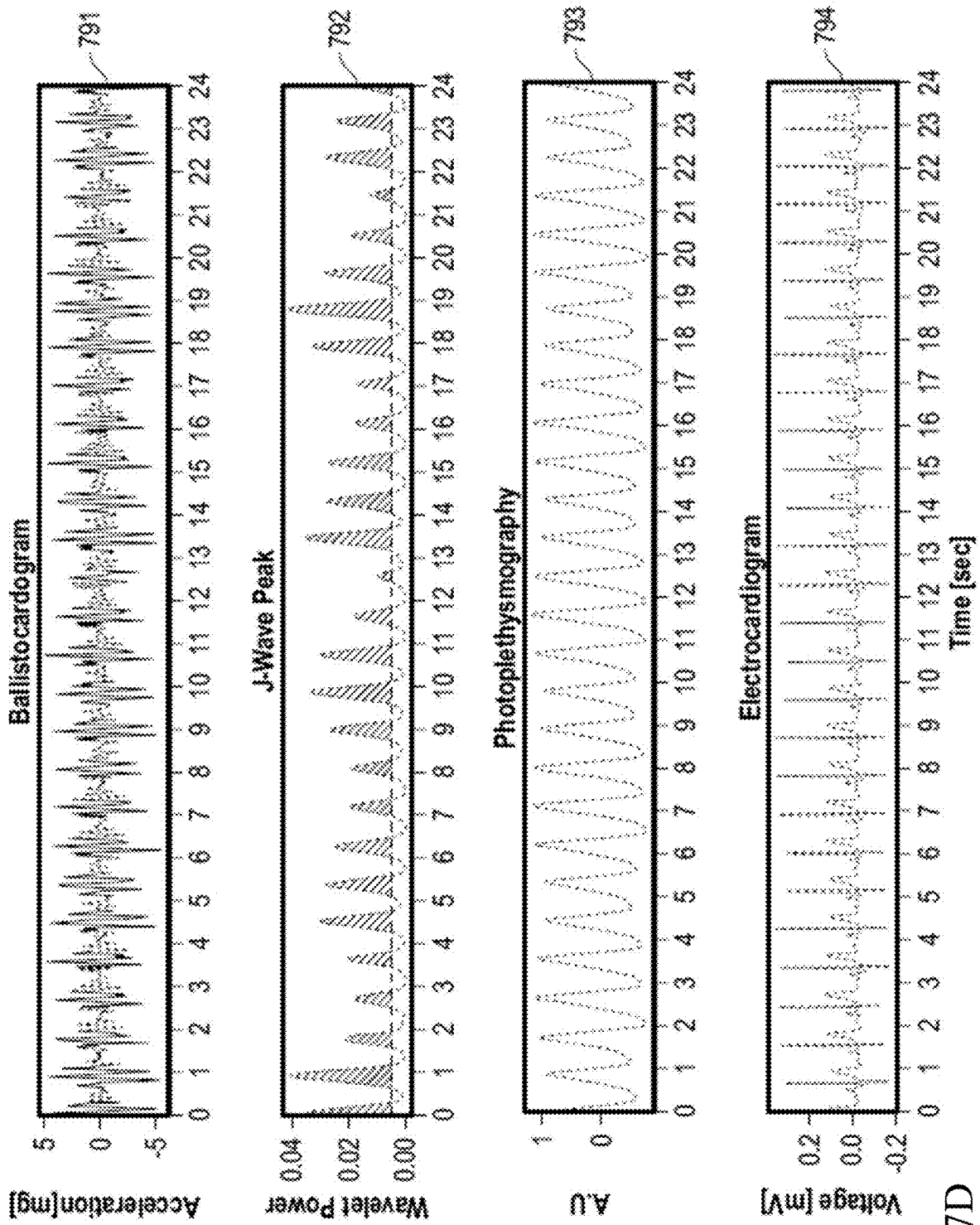


FIG. 7D

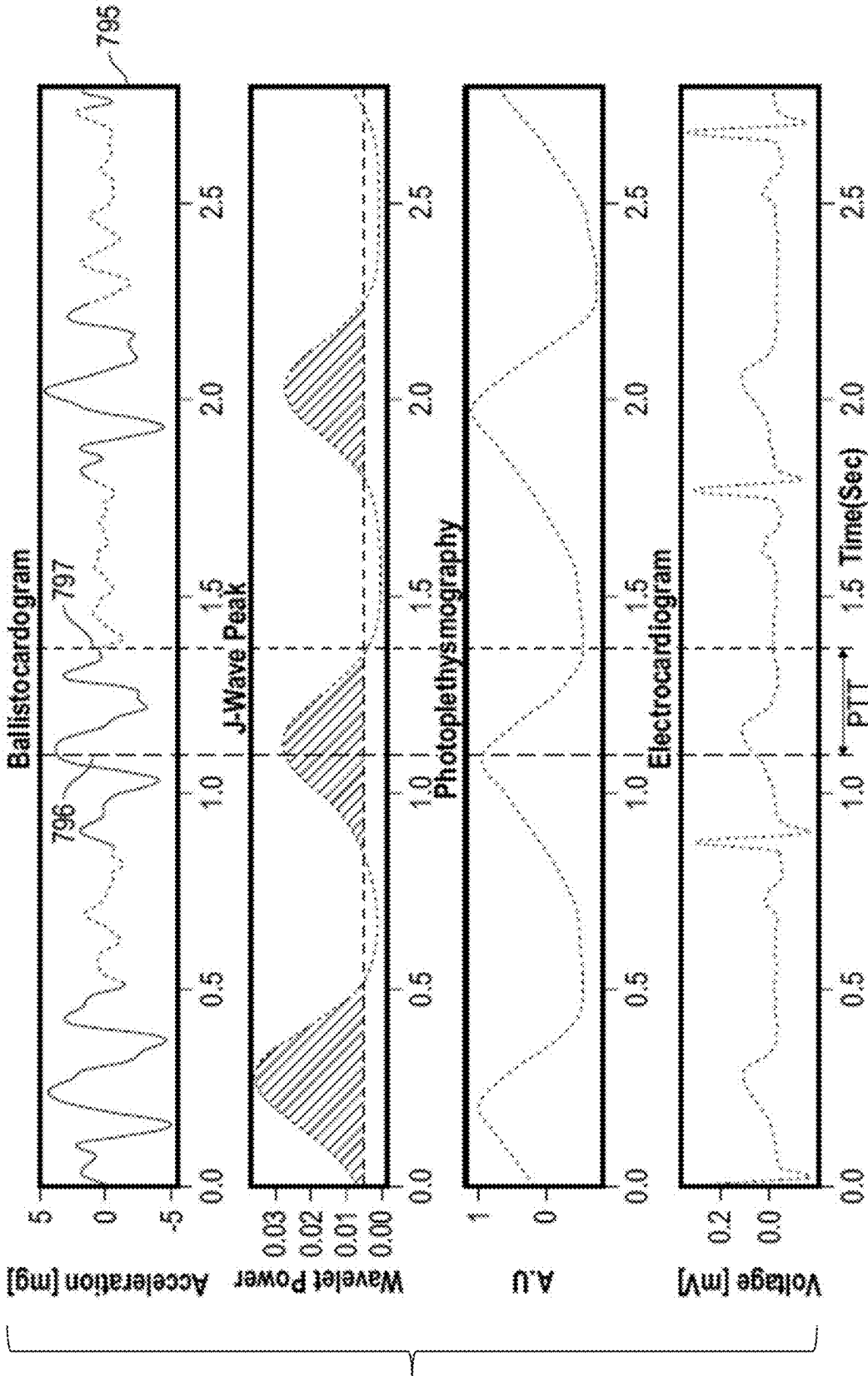


FIG. 7E

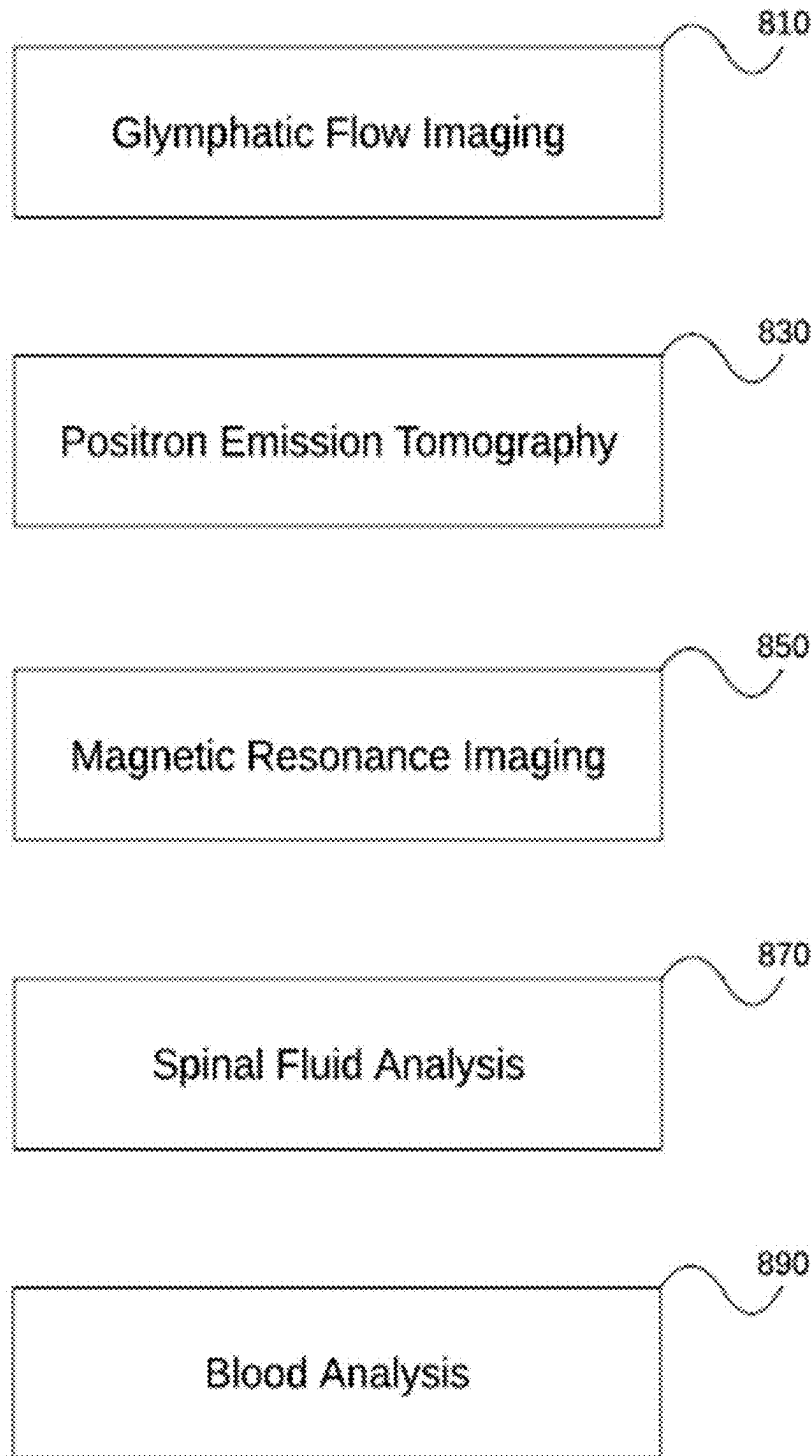


FIG. 8A

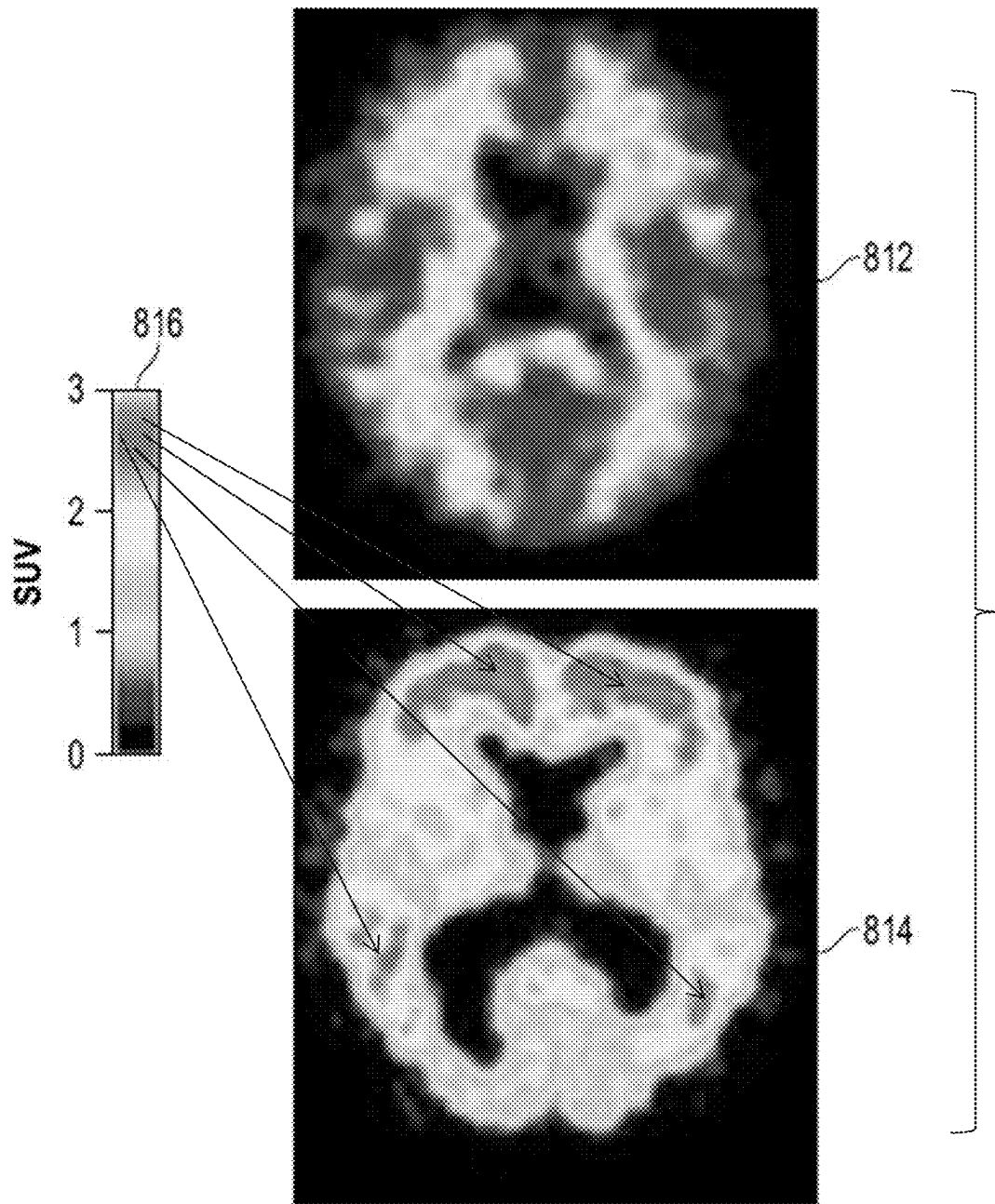


FIG. 8B

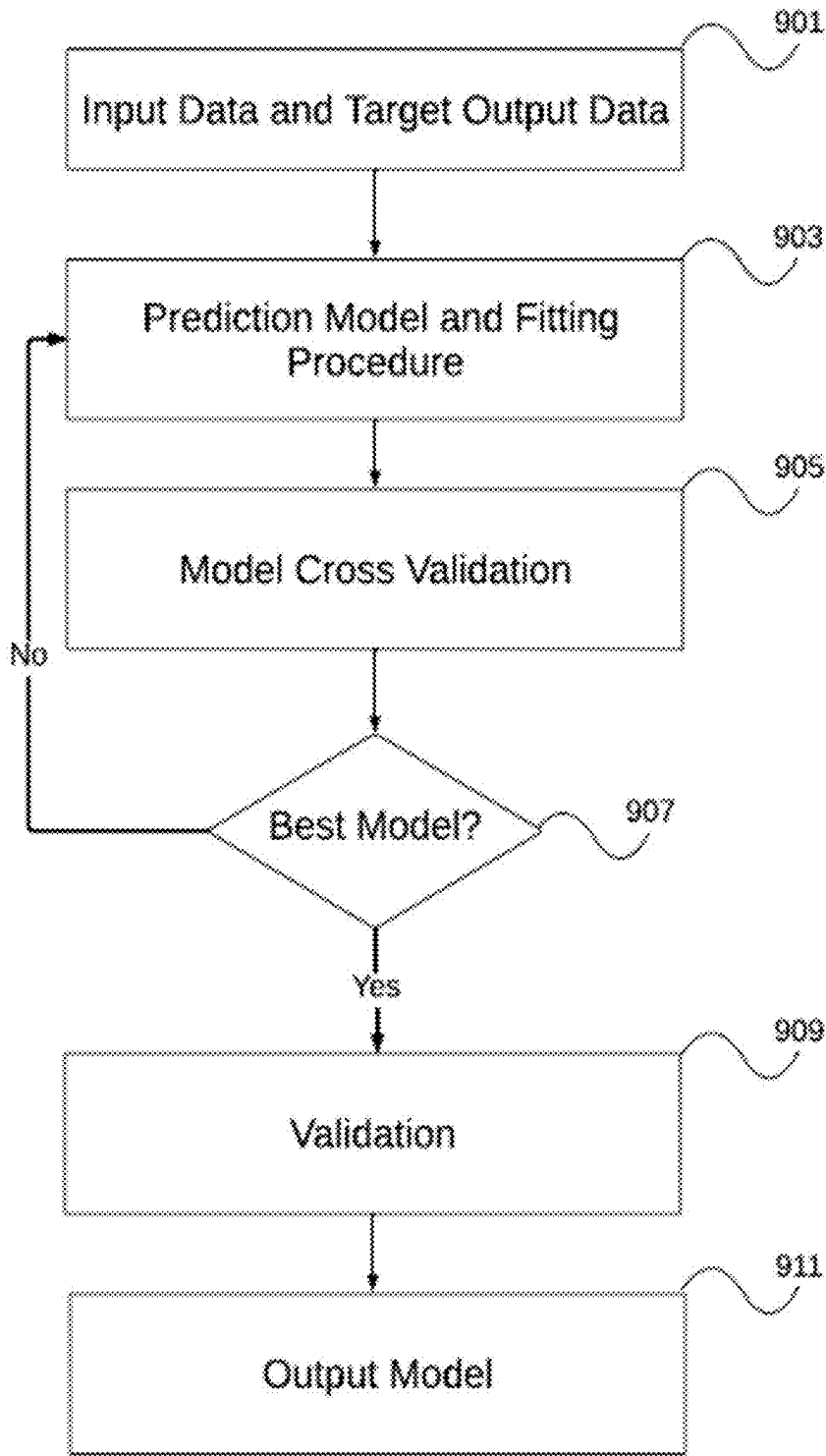


FIG. 9

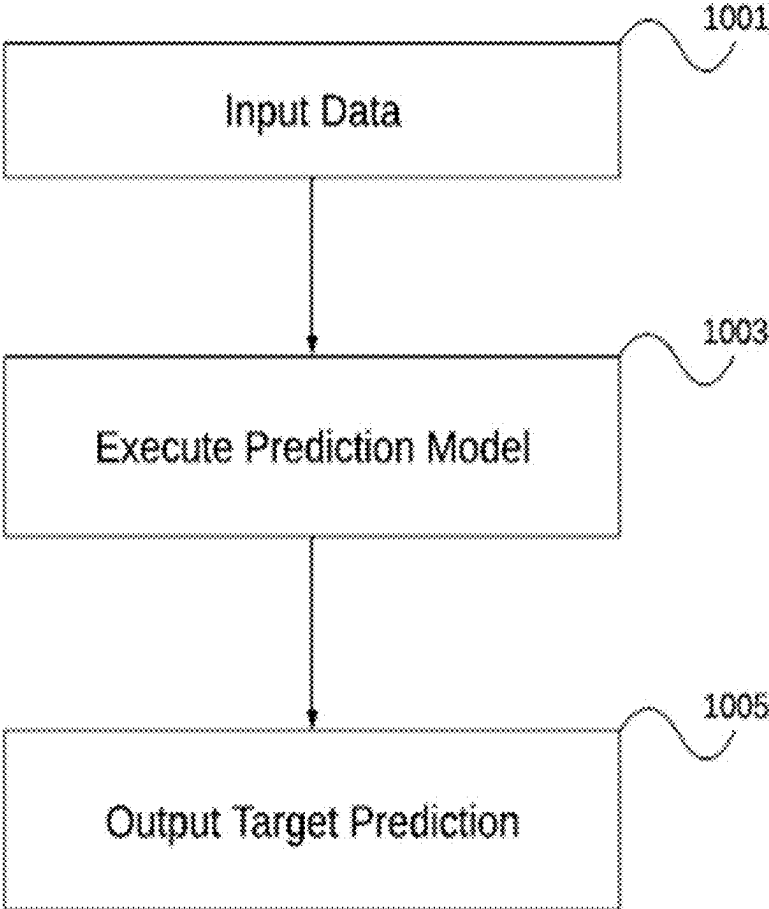


FIG. 10

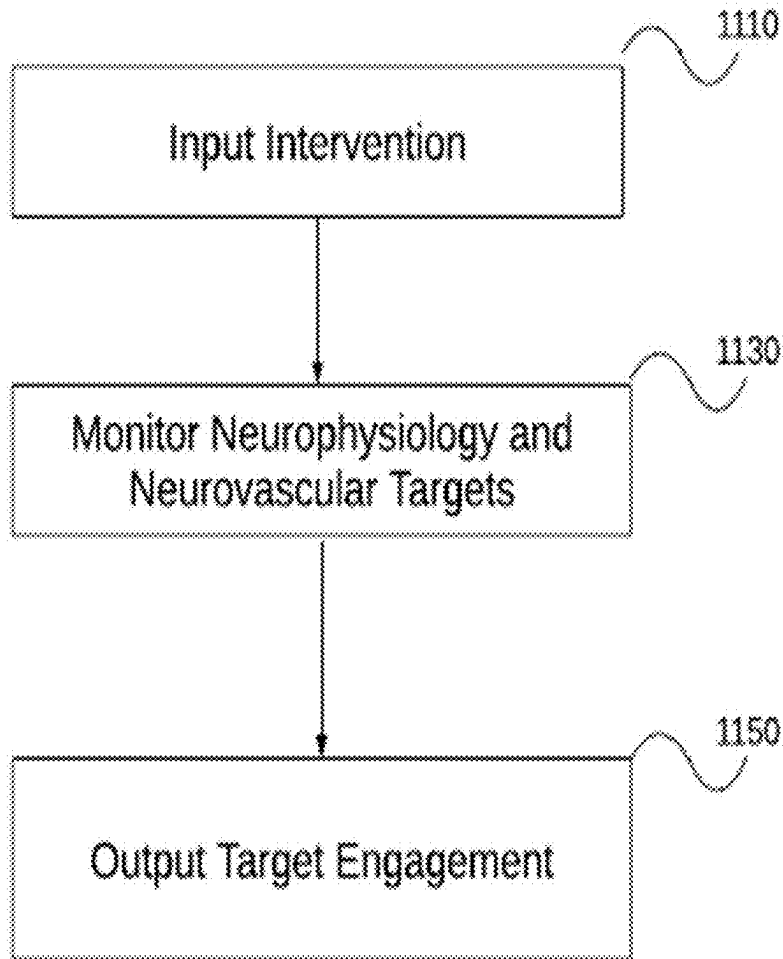


FIG. 11A

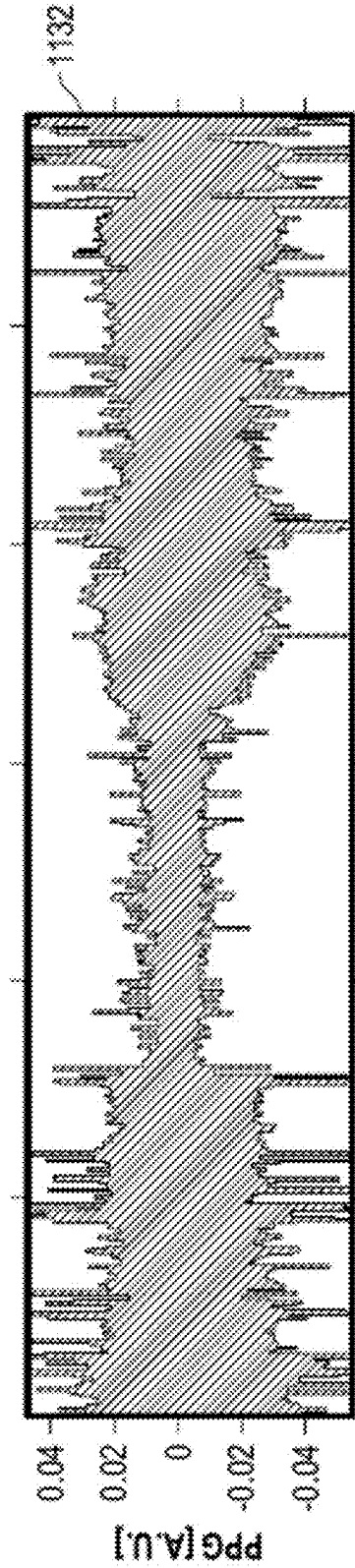
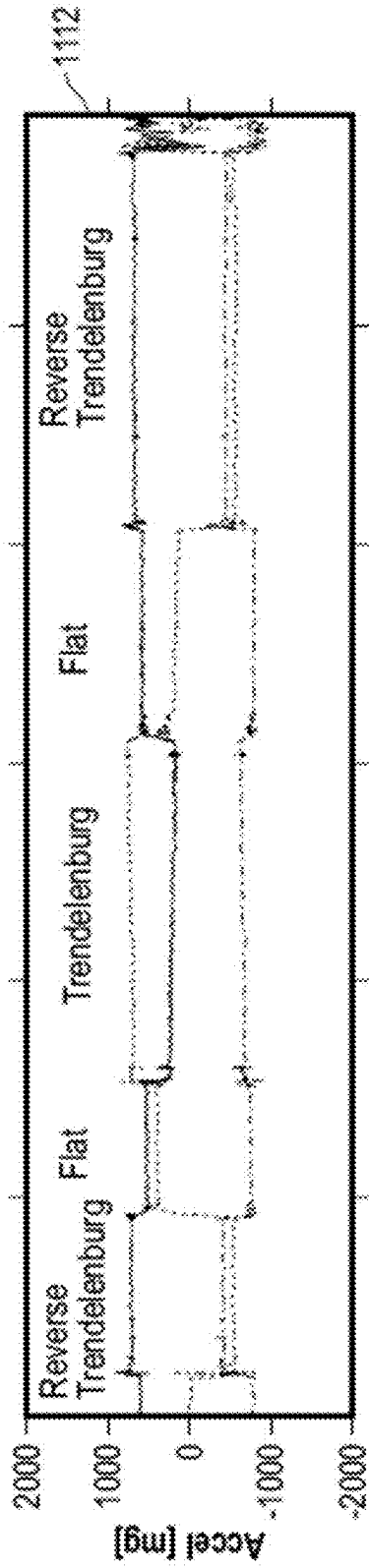
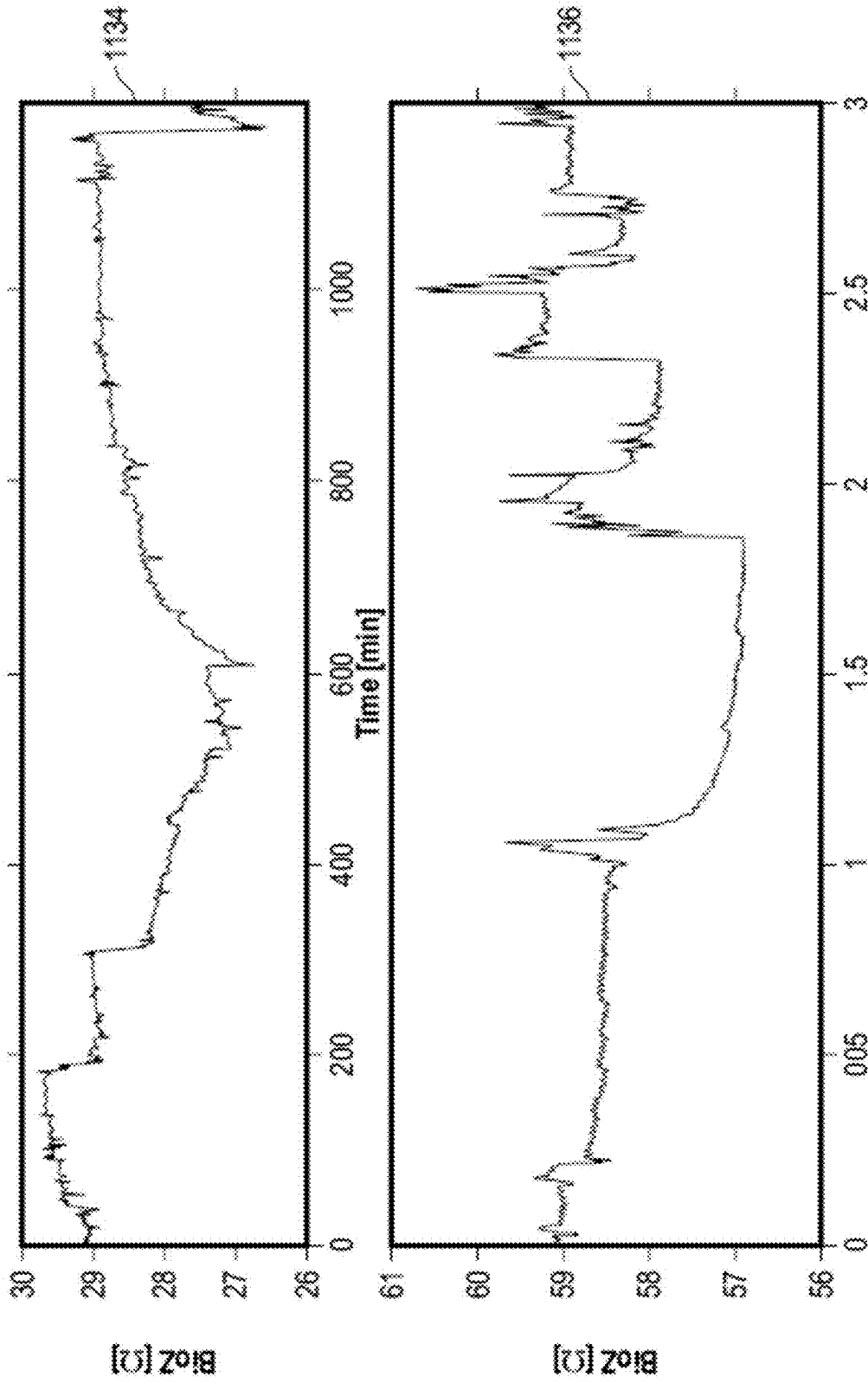


FIG. 11B



Time [min]  
FIG. 11B  
(Continued)

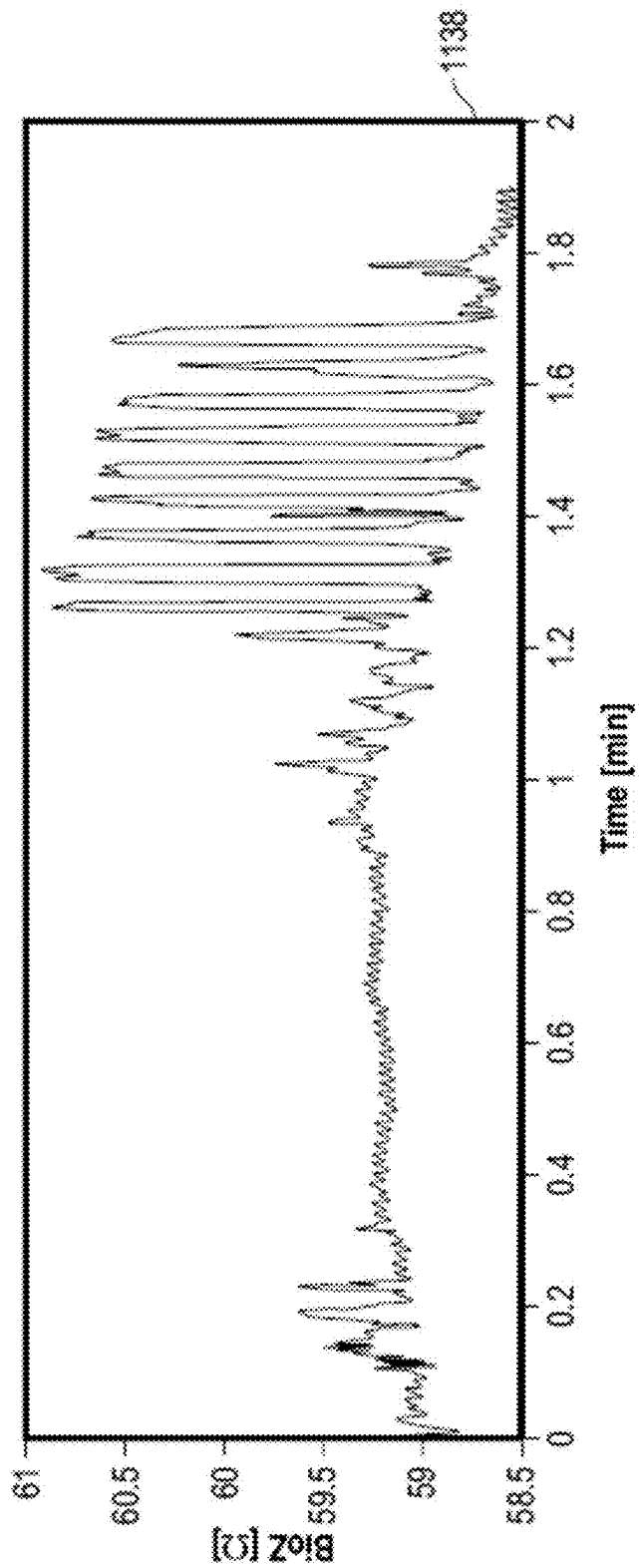


FIG. 11B  
(Continued)

1152

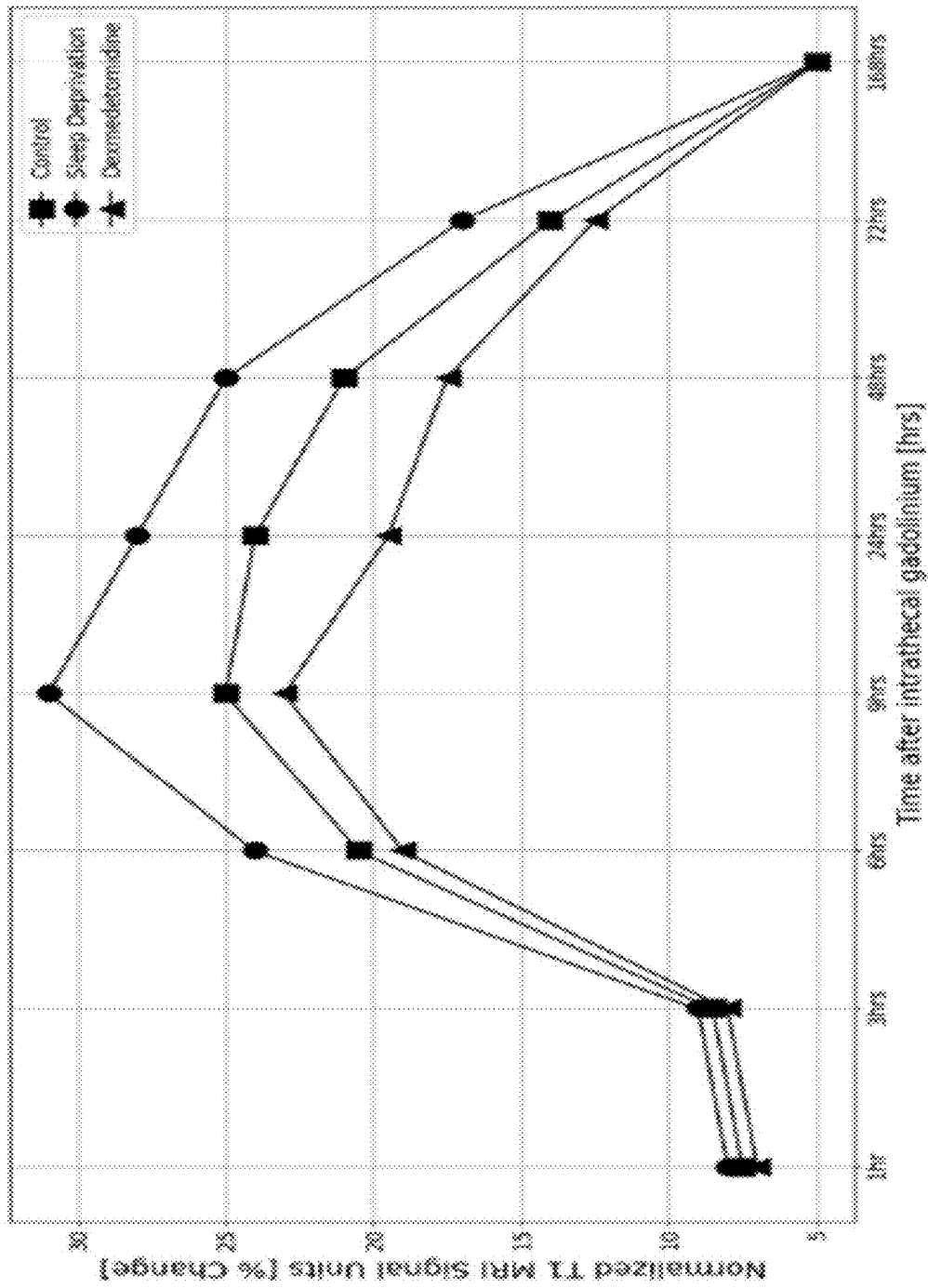


FIG. 11C

1

**NON-INVASIVE ASSESSMENT OF  
GLYMPHATIC FLOW AND  
NEURODEGENERATION FROM A  
WEARABLE DEVICE**

CROSS-REFERENCE TO RELATED  
APPLICATIONS

The present application is a continuation application of and claims priority to U.S. patent application Ser. No. 18/451,100 filed Aug. 17, 2023, which is a continuation application of and claims priority to U.S. patent application Ser. No. 17/937,952 filed Oct. 4, 2022, now U.S. Pat. No. 11,759,142, which is a continuation application of and claims priority to U.S. patent application Ser. No. 17/713,329 filed Apr. 5, 2022, now U.S. Pat. No. 11,478,184, which claims the benefit of U.S. Provisional Patent Application No. 63/244,080 filed Sep. 14, 2021. The entire content of the foregoing applications is incorporated herein by reference.

FIELD OF THE INVENTION

The invention relates generally to the collection of neurophysiology and neurovascular data from a wearable device for use in identifying, predicting, and treating neurodegeneration.

BACKGROUND

Interest in brain fluid transport systems has risen rapidly in recent years with the discovery of the glymphatic system and its role in brain protein clearance involved in neurodegeneration such as amyloid- $\beta$ . Inhibition of glymphatic flow accelerates protein accumulation and cognitive decline in animal models of Alzheimer's disease, traumatic brain injury and Parkinson's disease. The glymphatic flow is primarily active during sleep and driven by cerebrovascular arterial pulsations, thus, sleep, cerebrovascular integrity and neurovascular coupling are required for clearance of waste products that build up in the awake brain. A reduction in glymphatic flow results in accumulation of protein in the brain that leads to neurodegeneration (known as brain proteinopathy) and which can be detected with neuroimaging or molecular analyses of cerebrospinal fluid or blood plasma. Accordingly, non-invasive techniques for monitoring and analyzing information associated with glymphatic flow and its clearance of protein, with a focus on monitoring the mechanism of glymphatic flow that causes the protein accumulation rather than just reporting the accumulation of protein in the brain as done by neuroimaging or molecular analysis, can be useful in diagnosing and treating neurological degeneration.

SUMMARY

The present disclosure is generally directed to collecting neurophysiology and neurovascular data for use in identifying, predicting, and treating neurodegeneration. In one example embodiment, the disclosure is directed to a method, implemented with one or more computer processors, comprising: (a) accessing, by the one or more computer processors, neurophysiological data and neurovascular data recorded during sleep; (b) executing, by the one or more computer processors, a function mapping from said neurophysiological data and neurovascular data to a target that is a marker of glymphatic flow; and (c) outputting, by the one

2

or more computer processors, a target prediction model based on the function mapping.

In another example embodiment, the disclosure is directed to a system comprising: (a) one or more computer processors; (b) a neurophysiological data acquisition module configured to measure neurophysiological data; (c) a neurovascular data acquisition module configured to measure neurovascular data; and (d) a transmission module configured to transmit the electroencephalogram data and the neurovascular data to a second computing device.

The foregoing embodiments are non-limiting examples and other aspects and embodiments will be described herein. The foregoing summary is provided to introduce various concepts in a simplified form that are further described below in the detailed description. This summary is not intended to identify required or essential features of the claimed subject matter nor is the summary intended to limit the scope of the claimed subject matter.

BRIEF DESCRIPTION OF THE DRAWINGS

The specific features, aspects and advantages of the present invention will become better understood with regard to the following description and accompanying drawings where:

FIGS. 1A and 1B illustrate an embodiment of the system for non-invasive measurement of brain proteinopathy and neurodegeneration that is comparable to molecular analyses or neuroimaging configured in accordance with the present invention,

FIGS. 2A-2B illustrate an embodiment of the in-ear sensors of the system for non-invasive measurement of brain proteinopathy and neurodegeneration that is comparable to molecular analyses or neuroimaging configured in accordance with the present invention,

FIGS. 2C-2G illustrate the assembly process of the ear device that includes the flex circuit and manufactured soft-silicone components in accordance with the present invention.

FIG. 3 illustrates an example computing environment of the system for non-invasive measurement of glymphatic flow, brain proteinopathy, and neurodegeneration that is comparable to molecular analyses or neuroimaging configured in accordance with the present invention,

FIG. 4 is a functional description of the system in accordance with one embodiment of the present invention,

FIGS. 5A and 5B illustrate example methods associated with the collection of neurophysiology and neurovascular data from a wearable device for use in identifying, predicting, and treating neurodegeneration in accordance with one embodiment of the present invention,

FIGS. 6A-6F illustrate the neurophysiology data acquisition module and example associated data in accordance with one embodiment of the present invention,

FIGS. 7A-7E illustrate the neurovascular data acquisition module and example associated data in accordance with one embodiment of the present invention,

FIGS. 8A-8B illustrate the data acquisition module for a marker of glymphatic flow, a molecular analysis marker or a neuroimaging marker of neurodegeneration and associated images in accordance with an embodiment of the present invention,

FIG. 9 is the learning module of the function mapping from non-invasive neurophysiology and neurovascular input data to target output measurements of glymphatic flow in accordance with one embodiment of the present invention, or is the learning module of the function mapping from input

data for a marker of glymphatic flow to target output brain proteinopathy or neurodegeneration measurements from molecular analyses or neuroimaging, in accordance with another embodiment of the present invention,

FIG. 10 is the prediction module of a target marker of glymphatic flow from non-invasive neurophysiology and neurovascular input data in accordance with one embodiment of the present invention, or is the prediction module of a target molecular analysis or neuroimaging of brain proteinopathy and neurodegeneration using input data that are markers of glymphatic flow in accordance with another embodiment of the present invention,

FIGS. 11A-11C illustrate the target engagement module and associated data in accordance with one embodiment of the present invention.

#### DETAILED DESCRIPTION OF EXAMPLE EMBODIMENTS

Referencing the glymphatic flow responsible for the clearance of proteins described above, the perivascular spaces (PVS) of the brain are central to the glymphatic fluid transport system. Fluorescent dye-labeled particles that enable visualization of the perivascular spaces reveals that the system comprises periarterial, pericapillary, and perivenular spaces all interconnected into a single network. The glymphatic flow system clears brain interstitial fluid (ISF) waste products such as the proteinopathy proteins through the periarteriolar and perivenular spaces to meningeal lymphatics. The PVS is a site of great importance that is affected by disease processes such as cerebral amyloid angiopathy characterized by perivascular amyloid beta deposits and present in over 90% of Alzheimer's disease brains. PVS accumulation of p-tau is also observed in Alzheimer's disease and has been demonstrated to be present in arteries, arterioles and veins in the brain. In the glymphatic flow system, cerebrospinal fluid (CSF) enters the periarterial spaces, running in the direction of the blood flow and propelled by arterial wall pulsations. CSF mixes with ISF facilitated by aquaporin-4 (AQP4) water channels that are present at the vascular astrocytic endfeet forming the outer wall of the perivascular spaces. During sleep, arterial pulsations drive CSF bulk flow towards the brain. This process has been shown to be highly dependent on the arousal state and AQP4 expression. With modern neuroimaging techniques, it is now possible to visualize CSF flow and its clearance of proteins in the intact CNS by the second-to-second pulsatile movement of CSF through the ventricular system occurring with each cardiac contraction. Respirations further contribute to this rhythm, adding pulsations at a lower frequency. Superimposed on these acute pulsations is a circadian or diurnal rhythm with maximum CSF production occurring at night during sleep and minimum occurring in the afternoon. MRI studies in animal models using CSF tracers reveal that the glymphatic flow from ISF to subarachnoid CSF is enhanced during NREM sleep.

Sleep has profound effects on most aspects of brain physiology, including glymphatic flow and brain blood volume. In animal models, the amplitude of brain blood volume in non-rapid-eye movement (NREM) sleep doubles compared to the awake state and the amount of total blood volume in the brain changes significantly in the transition from wake to sleep and back to wake, showing that brain blood volume dynamics is coupled to arousal state. These changes in blood volume during sleep are linked to variations in neural activity which drive fluctuations in the

diameter of arterioles. The strength of this neurovascular coupling changes with arousal state, increasing substantially during sleep compared to wakefulness and explains the increase in brain blood volume during sleep when neural activity is lower than in the wake state.

The concentration of amyloid- $\beta$  and tau in the interstitial space and CSF follow a diurnal pattern with both protein concentrations reaching their peak during wakefulness and trough during sleep. A single night of sleep deprivation results in a significant increase in soluble amyloid- $\beta$  in the brain ISF demonstrated with positron emission tomography (PET) using an amyloid-binding radiotracer. The net concentration of amyloid- $\beta$ , tau and other proteins in the CSF and ISF reflect the combined effects of diurnal- and state-dependent variations in CSF production rate, ISF volume, ISF turnover rate, and glymphatic flow. Sleep slow-wave delta waves are associated with glymphatic flow and the amplitudes of slow delta waves responsible for effective waste removal during sleep. Sleep deprivation results in stalled glymphatic flow and the accumulation of waste solutes including amyloid- $\beta$  solutes and other proteins in the brain.

During sleep, glymphatic flow is increased by the action of astrocytes using AQP4 channels that are responsible for the modulation of phases between sleep and awake states. Using membrane channel protein AQP4 and water flux through AQP4, astrocytes can shrink the cell volume of brain parenchyma to increase ISF space by 23% during sleep enabling water and solutes to diffuse into adjacent perivascular spaces. During slow-wave sleep, the increase in ISF space, the opening of gap junction of astrocyte end-feet and an increase in cerebral hemodynamics creates an environment for exchange of nutrients and elimination of waste between ISF and CSF.

Damage to molecular and cellular components of the glymphatic flow system, to the brain neurovascular integrity and to its neurovascular coupling that occurs with aging, chronic co-morbidities, neurodegenerative diseases and physical brain trauma is closely linked to an increase of tau and amyloid- $\beta$  in extracellular fluids. The spread of these aggregated proteins in the brain parenchyma leads to worsening clinical symptoms and decline in cognition. Measuring the functional integrity of this system and the pathological accumulation of proteins in the brain ISF requires invasive procedures such as PET scans with radiotracers that bind to the protein of interest or lumbar puncture for CSF extraction and analysis of protein concentrations. The cost and complexity of these procedures limits their use to screen for brain proteinopathies or to monitor their progression. Without access to these tests, practitioners today use clinical assessment and cognitive evaluations to screen, diagnose and monitor neurodegenerative disorders such as Alzheimer's disease. The opportunity to intervene early in the 10-to-20-year pre-clinical period of these disorders is lost as is the ability to evaluate promising new treatments that could slow or stop disease progression. Another challenge with existing invasive test procedures is that they must be done in a hospital or clinic setting by trained technicians. This poses additional patient burden that further reduces the effectiveness of these expensive and time-consuming invasive procedures for monitoring progression of proteinopathy, adjusting care plans and monitoring response to new treatments.

The glymphatic system of protein waste clearance operates during sleep and is dependent on features measurable with sleep electroencephalogram (EEG) and on features that measure neurovascular blood volume, pulsation and coupling. Short term disruption in sleep causes an increase in

CSF and ISF waste proteins and long-term disruption leads to formation of ISF protein aggregates with neurodegeneration. A wearable device that can measure the relevant EEG features, brain blood volume changes and arterial pulsations during sleep, transmitting the data to a method and system that can predict CSF and ISF waste protein levels and ISF protein aggregation as can be measured using an existing invasive clinical procedure, would provide a significant advantage to medical screening and monitoring of neurodegenerative proteinopathy and help select appropriate interventions that slow or stop protein accumulation and neurodegeneration. As used herein and as described further below, a “wearable device” is a device worn by a subject comprising one or more sensors for collecting neurophysiological and/or neurovascular data from the subject, a processor, memory, and storage device for storing the collected data, and at least one wireless transmission module enabling the wearable device to transmit the collected data to another computing device. The wireless communication capability of the wearable device allows the wearable device to be self-contained so that it requires no external wiring to other equipment. The wearable device is configured to be worn by the subject while sleeping.

According to the embodiment(s) of the present disclosure, various views are illustrated in FIGS. 1A-11C and like reference numerals are being used consistently throughout to refer to like and corresponding parts of the example embodiments for all of the various views and figures of the drawing. Also, please note that the first digit(s) of the reference numbers in FIG. 1 and FIG. 4 correspond to the FIG. number in which the item or part is described in further detail.

The following detailed description contains many specifics for the purpose of illustration. Any one of ordinary skill in the art will appreciate that many variations and alterations to the following details are within scope of the disclosure. Accordingly, the following example embodiments are set forth without any loss of generality to, and without imposing limitations upon, the claimed invention.

Example embodiments of the present disclosure comprise a system and method that enables non-invasive measurement of brain proteinopathy and neurodegeneration. Such measurements are typically done in a medical facility using sophisticated equipment and involve a molecular analysis of cerebrospinal fluid or neuroimaging, and include proteinopathy proteins amyloid, tau or alpha-synuclein levels in a blood plasma or CSF assay, brain amyloid or tau load on a PET scan, brain atrophy on a structural brain MRI, repeated diurnal assessments to measure net change in proteinopathy protein CSF assay or soluble proteinopathy protein burden from neuroimaging. Example embodiments of the present disclosure teach a novel system and method that acquires sleep neurophysiology data synchronized with neurovascular data. The neurophysiology data includes electroencephalogram (EEG) data. The neurovascular data includes continuous transcranial impedance plethysmography (IPG), carotid pulse transit time (PTT), heart rate variability (HRV) and resting heart rate (RHR). The example embodiments can further perform the step of acquiring one of said molecular analyses or neuroimaging test of neurodegeneration following sleep and learning a function mapping from the sleep neurophysiology and neurovascular data to a molecular analyses or neuroimaging marker of neurodegeneration. Learning the function mapping includes using a loss function to determine relevant features in the sleep data, identifying a set of optimal weights that produce a minimum of the loss function, and creating a function mapping, also referred to as a brain proteinopathy and

neurodegeneration prediction model, using the optimal weights. The example embodiments can further include performing the step of applying the learned function mapping to new sleep neurophysiology and neurovascular data to screen for, or monitor, said molecular analyses or neuroimaging marker of neurodegeneration. The example embodiments can further include delivering a therapeutic intervention that targets an aspect of sleep neurophysiology or neurovascular either preceding sleep or during sleep, measuring target engagement or effect on the sleep neurophysiology and neurovascular, and further performing the step of applying the learned function mapping to predict the therapeutic effect on brain proteinopathy and neurodegeneration.

Another embodiment of the present disclosure comprises a system and method that enables a person to monitor the effect of a cardiovascular intervention or activity on a molecular analysis or neuroimaging marker of neurodegeneration, which embodiment teaches a novel system and method for performing the step of recording a cardiovascular intervention or activity data that precedes sleep, further performing the step of recording neurophysiology and neurovascular data during sleep and applying a learned function mapping to predict the therapeutic effect on brain proteinopathy and neurodegeneration of the cardiovascular intervention or activity.

Another embodiment of the present disclosure comprises a system and method that enables a person to monitor the effect of a pharmaceutical or neuromodulation intervention on a molecular analysis or neuroimaging marker of neurodegeneration, which embodiment teaches a novel system and method for performing the step of recording a pharmaceutical or neuromodulation intervention either preceding sleep or during sleep, further performing the step of recording neurophysiology and neurovascular data during sleep and applying a learned function mapping to predict the therapeutic effect on brain proteinopathy and neurodegeneration of the pharmaceutical or neuromodulation intervention.

Another embodiment of the present disclosure comprises a system and method that enables a person to monitor the effect of a diet intervention on a molecular analysis or neuroimaging marker of neurodegeneration, which embodiment teaches a novel system and method for performing the step of recording a diet intervention that precedes sleep, further performing the step of recording neurophysiology and neurovascular data during sleep and applying a learned function mapping to predict the therapeutic effect on brain proteinopathy and neurodegeneration of the diet intervention.

Another embodiment of the disclosure can be a wearable system comprising a wearable computer with sensors and a wireless communication interface to a mobile computer supporting a wireless network interface which communicates with a second computer including a network interface, each computer further including a processor, a memory unit operable for storing a computer program, an input mechanism operable for inputting data into said computer system, an output mechanism for presenting information to a user, a bus coupling the processor to the memory unit, input mechanism and output mechanism, wherein the wearable system includes various executable program modules stored thereon where when executed are operable to perform functions. The wearable computer with sensors can comprise a neurophysiology data acquisition module with sensors capable of recording EEG, a neurovascular data acquisition module with sensors capable of recording neurovascular data, with

the data stored on the wearable computer where when executed records to the memory unit of said wearable computer the neurophysiology and neurovascular sensor acquisition data. A transmission module can comprise a wireless network interface (e.g., a Bluetooth or WiFi radio) as well as instructions stored on said wearable computer where when executed transmit through the wireless network interface the recordings stored in the memory unit to said mobile computer. A second transmission module can also be stored on said wearable computer and comprise a wired network interface as well as instructions where when executed transmit through a bus network interface the recordings stored in the memory unit to a local computer station that further transmits the data to a second computer through a wireless network interface. A learning module can be stored on said second computer where when executed learns a function mapping from said transmitted recording to a molecular analysis or neuroimaging marker of neurodegeneration stored on said second computer, uses a loss function to determine relevant features in said recording, identifies a set of optimal weights that produce a minimum for said loss function, and creates said function mapping using said optimal weights. A brain proteinopathy and neurodegeneration prediction module can also be stored on said second computer where when executed applies the learned function mapping, also referred to as the brain proteinopathy and neurodegeneration prediction model, to a new transmitted recording of sleep neurophysiology and neurovascular sensor data from the wearable computer with sensors, to calculate a predicted value for the molecular analysis or neuroimaging marker of neurodegeneration from the new transmitted recordings. Thus, the brain proteinopathy and neurodegeneration prediction model can determine a predicted brain proteinopathy and neurodegeneration value from the new recording of data without requiring the invasive imaging or assay procedures described previously.

Another embodiment of the disclosure can be a wearable system comprising a wearable computer with sensors and a wireless communication interface to a mobile computer supporting a wireless network interface which communicates with a second computer including a network interface, each computer further including a processor, a memory unit operable for storing a computer program, an input mechanism operable for inputting data into said computer system, an output mechanism for presenting information to a user, a bus coupling the processor to the memory unit, input mechanism and output mechanism, wherein the wearable system includes various executable program modules stored thereon where when executed are operable to perform functions. In one embodiment, the wearable system can comprise a data acquisition module with sensors capable of recording cardiovascular activity data, with said data stored on the wearable computer where when executed records to the memory unit of said computer the acquisition data. In another embodiment, the wearable system can comprise a data input module capable of recording diet and nutrition data, with said data stored on the mobile computer where when executed records to the memory unit of said computer the data. In another embodiment, the wearable system can comprise a data input module capable of recording drug or neurostimulation data, with said data stored on the mobile computer where when executed records to the memory unit of said computer the data. In any of the preceding embodiments, a transmission module can comprise a communication interface and associated instructions stored on said wearable or mobile computer where when executed transmit through the wireless network interface the recordings stored

in the memory unit to said second computer. In any of the preceding embodiments, a module can be stored on said second computer where when executed applies a learned function mapping to said transmitted recording of sleep neurophysiology and neurovascular sensor data from the wearable computer with sensors, to calculate a value for a molecular analysis or neuroimaging marker of neurodegeneration from the transmitted recordings.

The details of the invention and various embodiments can be better understood by referring to the figures of the drawing. FIGS. 1A and 1B illustrate an embodiment of the functional description of the system configured in accordance with the present invention and is not intended to limit scope as one of ordinary skill would understand on review of this application that other configurations could be utilized without departing from the scope of the claimed invention. Referring to FIG. 1, the system can comprise a wearable device that can be attached to a subject's head. In one example, the wearable device can attach to the subject's ear. The wearable device can comprise the previously described neurophysiology and neurovascular data acquisition sensors **200** for non-invasive measurement. As further illustrated in FIG. 1, the wearable device can comprise a data storage, processing and transmission module **300** that stores the sensor data acquired, transforms the data to preliminary measurements of sensor impedance for determining that the sensors are correctly placed and the bladder is correctly pressurized, and can communicate with a mobile computer and/or a local computer, and/or a remote second computer to transmit the data for further processing into measurements of brain proteinopathy and neurodegeneration that are comparable to molecular analyses or neuroimaging markers. The non-invasive sensors **200** are connected to module **300** through a form-fitting band **100** that houses electrical conduits, electronically isolating digital from analog sensor signals, an air tube that connects an air bladder in sensor **200** with a piezoelectric pump in **300** and inflates the in-ear portion of the ear device **200** to ensure adequate interfacial contact between the surface sensors and the ear and canal epidermis, and a nitinol band designed to ensure secure fitting of the wearable device. An illustration of the attached device is shown in **110**. It should be understood that in alternate embodiments the components of the wearable device can have other configurations and can attach to the user with other mechanisms. For example, the air bladder can be replaced by another type of bladder that fills with fluid.

FIGS. 2A-2B illustrate an embodiment of the ear sensors of the system configured in accordance with the present invention and are not intended to limit scope as one of ordinary skill would understand on review of this application that other configurations could be utilized without departing from the scope of the claimed invention. Referring to FIG. 2(a), the flex circuit housed by the ear device **200** is illustrated in **210**. Component **212** illustrates positioning of the inertial measurement unit (IMU) that measures milligravitational acceleration capable of perceiving ballistic acceleration in the ear from the blood ejected into the aorta with each cardiac contraction. Component **214** illustrates positioning of the photoplethysmogram (PPG) sensor on the flex circuit so that it is in contact with the ear canal wall. The PPG through measuring the reflection of two wavelengths of infrared light through the ear canal skin is capable of measuring pulsatile changes of ear capillary blood volume with each heart beat and arterial oxygen saturation. Flex circuit leads **216** are terminated on the surface of the ear device **200** to be in contact with two conductive electrodes

covering the ear device that can be conductive ink, fabric or other material. Referring to FIG. 2(b) providing illustration 220, the 1-layer sections of the flex circuit are designed to flex naturally to accommodate for differences in user ear anatomy, the second layer of the 2-layer sections of the flex is a stiffener applied to the undersurface of the flex circuit to keep the sections stiff so that the active and passive electronic components do not detach with bending, and the 4-layer section has a grounding plane between analog and digital signals to reduce or eliminate electronic coupling resulting in signal corruption.

Referring to FIGS. 2C-2G, the illustrations 230, 240, 250, 260 and 270 show the assembly process of the ear device that includes the flex circuit 210 and manufactured soft-silicone components illustrated in 230 and 250. Illustration 240 shows the flex circuit 242 attached to the silicone component 230. Illustration 250 shows the bladder 252 in the second silicone component that is pressurized, with air or fluid, once inside the ear canal. Through inflation, the PPG sensor 264 is brought into tight contact with the ear canal skin for improved signal-to-noise measurement and further ensures good interfacial contact between the conductive electrodes 272 and 273, used to measure the neurophysiology electrical currents from the brain and the transcranial bioimpedances, and the ear canal epidermis. Note the ergonomic bend in the second silicone component 252 that mimics the first bend in the human ear-canal. The positioning of the IMU 262 on the device is illustrated in FIG. 2F.

FIG. 3 illustrates an embodiment of the previously described wearable device illustrated as wearable computing device 305, comprising the data storage, processing and transmission module 300 configured in accordance with the present invention and is not intended to limit scope as one of ordinary skill would understand on review of this application that other configurations could be utilized without departing from the scope of the claimed invention. Specifically, the data storage, processing, and transmission module 300 comprises one or more processors 308, a memory 310, a storage device 314, and a transmission module 312. The components of the data storage, processing, and transmission module 300 are responsible for storing the ear device sensor data, processing the data into preliminary measures of sensor impedance to determine that the sensors are correctly placed and the bladder is correctly pressurized, and transmitting the data for further off-line processing into measurements of brain proteinopathy and neurodegeneration that are comparable to molecular analyses or neuroimaging markers. The example of the wearable computing device 305 in FIG. 3 also illustrates the previously described sensors 200, such as an IMU and/or PPG, which gather data when positioned in the ears of a patient and which provide the data for storage in the storage device 314, processing by the processor 308, and transmission by the transmission module 312. The input/output device 314 can be a user interface in the form of buttons or a display screen. In other embodiments of the wearable computing device, the input/output device may be omitted.

The example embodiment of FIG. 3 illustrates the wearable computing device 305 capable of wireless communication via wireless links with a mobile computing device 320, such as a smartphone or tablet, and a local computing device 340, such as a desktop computer. It should be understood that it is not a requirement to have both a mobile computing device and a local computing device and in alternate embodiments only one of the mobile computing device 320 and local computing device 340 may commu-

nicate with the wearable computing device 305. As illustrated in FIG. 3, the mobile computing device 320 and the local computing device 340 comprise conventional components that are readily understood, including a processor 322/342, memory 324/344, a transmission module 326/346, an input/output interface 328/348, and a storage device 330/350. One or both of the mobile computing device 320 and the local computing device 340 can transmit the data collected by the wearable computing device 305 to a second computing device 360. The second computing device is typically located remotely and accessed via a wide area network such as the Internet. The second computing device can comprise computing components, such as a processor 362, memory 364, transmission module 366, input/output interface 368, and storage device 370. The storage device 370 can store various program modules that are executable by the processor 362. Specifically, the storage device 370 can comprise a learning software module and a prediction software module. For example, the learning software module can comprise a machine learning algorithm or deep learning algorithm that determines a function mapping from the collected neurophysiological and neurovascular data to a target marker of glymphatic clearance or neurodegeneration. The prediction module can comprise a model based on the function mapping that is used to predict glymphatic clearance or neurodegeneration based on sensor data that is newly collected by the wearable computing device from a patient.

FIG. 4 illustrates an embodiment of the functional description of the system configured in accordance with the present invention and is not intended to limit scope as one of ordinary skill would understand on review of this application that other configurations could be utilized without departing from the scope of the claimed invention. Referring to FIG. 4, a user's sleep neurophysiology data is captured and recorded by the neurophysiology data acquisition module 600 through sensors positioned on the user's head, such as the previously described sensors positioned in the ear. The neurovascular data acquisition module 700 further captures the user's sleep neurovascular data through sensors positioned on the user's head. As explained previously, the neurophysiology data acquisition module 600 and the neurovascular data acquisition module 700 can be implemented in the wearable device.

In contrast, the brain proteinopathy and neurodegeneration target data acquisition module 800 is an invasive module typically implemented using sophisticated equipment at a medical facility and is responsible for acquiring one or more molecular analysis or neuroimaging markers of neurodegeneration. The marker of interest can be a CSF or plasma assay of one of several brain proteinopathy proteins including amyloid beta 42, tau, alpha-synuclein and neurofilament light that are markers of neurodegenerative disorders, a neuroimaging scan such as PET scan with a radiotracer for the protein of interest, an MRI with contrast agent to measure brain atrophy. The CSF assay or PET scan can be taken after sleep to assay an existing level of CSF protein or protein build up in the brain, or taken both before and after sleep to assay the net change in the protein level that occurred during sleep. The marker can also be an MRI with intrathecal contrast agent injected into the CSF prior to sleep and which is cleared via brain interstitial fluid transport into the meningeal lymphatic and cavernous sinus system during sleep, and the uptake and clearance rate measurable using repeat MRI scanning.

The target marker data measured by module 800 is used by the target learning module 900 to create a target predic-

tion module **1000** that maps new neurophysiology data from module **600** and new neurovascular data from module **700** to a predicted molecular or neuroimaging marker of neurodegeneration for longitudinal monitoring without needing to repeat the invasive measurement of module **800**. The target learning module **900** and target prediction module **1000** can be implemented as software that uses a machine learning or deep learning algorithm to provide an output. The target learning module **900** and target prediction module **1000** can be implemented as software executed on one or more remote computers such as the second computer described previously. Target prediction module **1000** can also map sleep neurophysiology data from module **600** and sleep neurovascular data from module **700** taken from a new patient to a molecular or neuroimaging marker of neurodegeneration for non-invasive screening that can be used in medical decision making to evaluate the need for the invasive measurement of module **800**. The target engagement module **1100** measures the effect that a putative therapeutic intervention has on the sleep neurophysiology or neurovascular data, or degree of target engagement, and how that effect translates into a change in the predicted molecular or neuroimaging marker of neurodegeneration. The intervention can be one of cardiovascular, diet, sleep, pharmacological or neurostimulation.

FIGS. **5A** and **5B** illustrate embodiments of the present invention in the form of two methods and are not intended to limit scope as one of ordinary skill would understand on review of this application that other methods could be utilized without departing from the scope of the claimed invention. Referring to FIG. **5A**, a method of creating and applying a target prediction model is illustrated. Beginning with operation **505**, a processor of a computing device accesses neurophysiological and neurovascular data recorded while one or more patients were sleeping. The data can be recorded using the previously described wearable device or using other devices. In operation **510**, the processor can use a learning software module to determine a function mapping between the recorded data accessed in operation **505** and target marker data. The learning software module can use a machine learning algorithm to determine the function mapping. The target marker data can be data indicating glymphatic flow within the brain. Alternatively, the target marker data can be one of a molecular analysis marker of neurodegeneration or a neuroimaging marker of neurodegeneration such as those described in association with module **800** of FIG. **4**. After completing the function mapping, in operation **515** the learning software module outputs a target prediction module. The example method of FIG. **5A** can end after operation **515** because the target prediction module can be used in a variety of ways. However, the example method of FIG. **5A** continues with operations **520-530** to illustrate one application of the target prediction module. Specifically, in operation **520**, neurophysiological and neurovascular data that is newly collected from a patient using the wearable device can be input into the target prediction model to generate a marker of glymphatic clearance or a marker of neurodegeneration. In operation **525**, the marker that is output can be used to determine and administer a therapeutic intervention for the patient. In certain embodiments, information pertaining to the therapeutic intervention can be input into the wearable device. Lastly, after the therapeutic intervention has been administered, the wearable device can be used again in operation **530** to collect new data from the patient to determine the efficacy of the therapeutic intervention.

Referring now to FIG. **5B**, an example method for operating a wearable device in accordance with the example embodiments of this disclosure is illustrated. Beginning with operation **550**, the neurophysiological and neurovascular data sensors of the wearable device can be activated for gathering data while a patient sleeps with the wearable device attached to the patient's ears. For example, the processor of the wearable device can execute a data acquisition module stored in the wearable device's storage module, wherein the data acquisition module controls the operation of the sensors. In operation **555**, the sensors of the wearable device, such as the IMU and/or PPG, gather neurophysiological and neurovascular data while the patient sleeps. In operation **560**, the wearable device can store the gathered data in the storage device of the wearable device. In some instances, as indicated in operation **565**, the wearable device's processor can perform certain initial signal processing on the data gathered by the sensors and store such processed data in the wearable device's storage device. Lastly, in operation **570**, the transmission module of the wearable device can manage the transmission of the gathered and/or processed data from the wearable device via a wired or wireless communication link to one or both of a mobile computing device and a local computing device. The mobile computing device and/or local computing device can relay the data from the wearable device to a second computing device that can execute a learning software module and a prediction software module.

FIGS. **6A-6F** illustrate an embodiment of the neurophysiology data acquisition module **600** of the system configured in accordance with the present invention and is not intended to limit scope as one of ordinary skill would understand on review of this application that other configurations could be utilized without departing from the scope of the claimed invention. Referring to FIG. **6A**, in **610** raw EEG data is acquired from the user during sleep. The EEG data can be acquired using conventional EEG headcap sensors with a bedside amplifier for recording the signals, or using a wearable device with integrated electronics for amplifying and recording the signal. From the raw EEG signal, various derivations can be analyzed to generate a hypnogram **620** that marks the four stages of sleep, N1, N2, N3 and rapid eye movement (REM) from which additional sleep performance parameters **680** can be derived including total sleep time, sleep onset latency, wake after sleep onset, sleep efficiency and number of awakenings. In **630**, slow wave oscillations in the raw EEG signal are detected and the density (number per minute), amplitude and duration of these oscillations are reported in 30 or 60 second epochs during sleep. In **640**, slow wave activity defined as the relative or absolute power in the EEG signal in the frequency band between 0.5 Hz and 4.5 Hz is computed for every 30 or 60 second epoch and reported. Options for computing the power spectrum include a fast Fourier transform, Welch's periodogram or the multitaper method. In **650**, another sleep EEG element, sleep spindles, are detected in one or more EEG derivations. Sleep spindles occur in two types, fast and slow, depending on the spindle frequency. Spindle density, frequency, duration and amplitude is reported in 30 or 60 second epochs for each type. Both slow wave oscillations or activity, **630** and **640**, and sleep spindles **650** are sleep microstructure markers of glymphatic flow. Finally, in **670** the full power spectral density in the EEG signal is computed in 30 or 60 second epochs and reported.

One or more of the EEG data elements illustrated in FIG. **6A** can be used in connection with the target prediction model. For example, the EEG data elements illustrated in

FIG. 6A can be used to train the target prediction model. As another example, if the EEG data elements are data that is newly collected after the target prediction model is trained, the EEG data elements can be input into the target prediction model to predict new target markers of neurodegeneration.

Referring to FIG. 6B, 622 is an example sleep hypnogram from an individual during one night EEG recording using a standard 10-20 scalp wet-sensor montage and the results of a C3 to M1 derivative is shown. The sleep hypnogram shows when the individual was awake (W) and in stage N1, N2, N3 or REM sleep in each 30 second epoch. In 642 is illustrated the slow wave activity in the 0.5 to 4.5 Hz bandwidth using a Welch periodogram in 30 second epochs. The slow wave activity is seen to peak during N3 sleep. Important features of the slow wave activity include duration, power and frequency that can be used in connection with the target prediction model. For example, the features of the slow wave sleep elements illustrated in FIG. 6B can be used to train the target prediction model. If the EEG slow wave sleep elements are data that is newly collected after the target prediction model is trained, the EEG slow wave sleep data elements can be input into the target prediction model to predict new target markers of neurodegeneration.

During the same night and for the same individual, simultaneous recordings were made using an ear device comprising modules 100, 200 and 300 illustrated in FIG. 1A. In FIG. 6C, 624 shows the sleep hypnogram recorded by the ear device and 644 shows the slow wave activity in the 0.5 to 4.5 Hz bandwidth using a Welch periodogram and 30 second epochs.

Referring to FIG. 6D, for the same individual during the same night of EEG recording, sleep microstructure spindle activity in the 10 to 16 Hz bandwidth using a Welch periodogram in 30 second epochs are illustrated in 652 from the standard 10-20 scalp wet-sensor montage using a C3 to M1 derivative. In 654 is illustrated the same analysis using the sensors from the ear device comprising of modules 100, 200 and 300 illustrated in FIG. 1A. In both illustrations, peak spindle activity is seen to coincide with stage N2 sleep. Important features of spindle activity include duration, power and frequency. For example, the features of the sleep spindle elements illustrated in FIG. 6D can be used to train the target prediction model. If the EEG sleep spindle elements are data that is newly collected after the target prediction model is trained, the EEG sleep spindle data elements can be input into the target prediction model to predict new target markers of neurodegeneration.

For the same individual during the same night of EEG recording, FIG. 6E illustrates the sensitivity agreement on hypnogram stages and sleep performance parameters between different EEG electrode positions. Illustrated in 682 of FIG. 6F are the sensitivity agreement of hypnogram stages between the C3 to M1 derivative to score the hypnogram and the derivative between the left and right ear electrodes in FIG. 1A illustrated in 200. Illustrated in 684 of FIG. 6F are the agreement in sleep performance parameters derived from the sleep hypnograms between the C3 to M1 derivative to measure the hypnogram and the derivative between the left and right ear electrodes in FIG. 1A illustrated in 200. The differences in sensitivity agreement and performance parameters are due to the anatomical differences in the sensor location for measurement highlighting the importance of consistent anatomical sensor placement between uses and across users to extract sleep EEG features for the training the target prediction model and as new inputs to a trained target prediction model to make predict new target markers of neurodegeneration. In-ear lead placement

as done by the wearable ear device illustrated in FIG. 1A using anatomically informed ear fittings shown in FIGS. 2C-2G ensure consistent anatomical placement by a user.

FIG. 7A-7E illustrates an embodiment of the neurovascular data acquisition module 700 of the system configured in accordance with the present invention and is not intended to limit scope as one of ordinary skill would understand on review of this application that other configurations could be utilized without departing from the scope of the claimed invention. Referring to FIG. 7A, the same sensors 272 and 273 illustrated in FIG. 2G used for recording in-ear EEG are multiplexed to record at 80 kHz, well above EEG bandwidth, transcranial impedance from left to right ear during sleep. Transcranial impedance tracks fluid changes in the brain that arise during sleep, for example from sleep related changes in glymphatic flow and cerebral spinal fluid production, illustrated in module 710, and from cardiac pulsations, leading to a beat-to-beat measurable cerebral perfusion pulsation illustrated in module 730. With each heartbeat, a large fraction of the cardiac output is ejected into the internal carotid and vertebral arteries and delivered to the brain parenchyma. This change in brain blood volume lowers the transcranial impedance and is measurable by the sensors. The amplitude of the impedance waveform and the numerical integration of the impedance waveform pulse are proportional to the volume of blood that is ejected into the brain during that cardiac cycle. The moving average of the transcranial impedance during sleep drifts lower. This drift corresponds to a diurnal fluctuation in brain fluid volume with increased fluid volume during sleep from, for example increases in glymphatic flow and cerebral spinal fluid production, and is measurable by module 710. A larger drop between onset of sleep and the sleep nadir of the transcranial impedance correlates with a larger increase in total brain fluid composition that would be expected with greater glymphatic flow. The pulsations recorded by module 730 assist fluid flow through the brain interstitial spaces that promotes glymphatic flow during sleep and protein clearance. The larger magnitude of these pulsations, measured as either their amplitude or numerically integrated area measuring ejection volume, is expected to propel greater glymphatic flow leading to improved clearance. Photoplethysmography sensors located in the ear on the device illustrated in FIG. 1A and illustrated 264 in FIG. 2F, record heart rate variability during sleep in module 750, resting heart rate by module 770 and sinus arrhythmia that can be used to estimate breathing rate also by module 770. Heart rate variability during sleep measures the sympathetic-parasympathetic tone of the autonomic nervous system, with lower heart rate variability indicating lower parasympathetic tone and higher sympathetic tone. During sleep, higher sympathetic tone activated by the locus coeruleus in the brain decreases brain interstitial fluid flow and protein biomarker clearance. Higher sleep heart rate variability is expected to lead to greater glymphatic flow and protein clearance. Lower sleep resting heart rate recorded by module 770 is compensated by higher cardiac stroke volume to maintain a tightly regulated cerebral blood flow. A higher cardiac stroke volume results in larger cerebral perfusion pulsations that are measurable by module 730 and increase the propelling forces of glymphatic flow. Conversely, diseases that harden arteries, in particular the arterioles that penetrate the brain parenchyma alongside which run the perivascular spaces containing cerebrospinal fluid that is propelled into the brain parenchyma to drive glymphatic flow, decrease the propelling forces. A decrease in the propelling force is measured by a decreases in the magnitude of the cerebral perfusion pulsa-

tion in module **730**. Changes in respiratory rate recorded in module **770** also alters the blood volume pulsations in **730** by affecting venous return to the heart and thereby changing cardiac stroke volume.

One or more of the neurovascular data elements illustrated in FIG. **7A** can be used in connection with the target prediction model. For example, the neurovascular data elements illustrated in FIG. **7A** can be used to train the target prediction model. As another example, if the neurovascular data elements are data that is newly collected after the target prediction model is trained, the neurovascular data elements can be input into the target prediction model to predict new target markers of neurodegeneration.

Referring to FIG. **7B**, **714** shows a sleep recording of the cerebral fluid volume from the transcranial impedance sensors illustrated by **272** and **273** in FIG. **2G** for the left in-ear device. The sleep hypnogram illustrated in **712** corresponds to the recorded impedance **714** and shows the decrease in impedance as the patient progresses to deep sleep in stage N2 and N3 (slow wave sleep). The drop in impedance corresponds to an increase in fluid (or water) composition in the brain that corresponds to increase in glymphatic flow through the brain tissue and an accompanying increase in the production of cerebrospinal fluid.

An interval of cerebral perfusion pulsation during sleep for this patient is illustrated in **732** and the corresponding ECG signal in **734**. The cerebral perfusion stroke volume is the difference in impedance between the peak and the trough of a pulsation. A larger difference signifies a greater change in fluid, or water, composition resulting from the heart beat and correlates directly with cerebral stroke volume.

Referring to FIG. **7C**, for each 500 second epoch during sleep, the sleep hypnogram is illustrated in **752**, a recording of resting heart rate by module **770** is illustrated in **754** and a recording of resting heart rate variability by module **750** is illustrated in **756**, where in both **754** and **756** are illustrated the recording from the sensors by the wearable device illustrated in FIG. **1A** against gold-standard electrocardiogram (ECG) recordings.

Referring to FIG. **7D**, the pulse transit time module **790** records a ballistocardiogram (BCG) **791** from the in-ear inertial measurement unit (IMU) illustrated by **262** in FIG. **2F**. The BCG I, J and K waveforms are highlighted in the recording **791**. Using a wavelet analysis of the BCG recording, the power of the J waveform is illustrated in **792**, with its peak aligning with the J waveform peak of the BCG. Illustrated in **793** is the PPG waveform recording from the in-ear sensor **264** illustrated in FIG. **2F** and **794** illustrates the ECG recording. The IMU, PPG and ECG recordings are time-synchronized by module **790**. A 2.5 second duration close-up of the data illustrated in **791-794** is illustrated in **795** of FIG. **7E**. Computation of the pulse-transit time of a cardiac ejection is illustrated in **795**. The maximum blood acceleration is marked by the BCG J-wave **796** and trough of the PPG waveform **797** corresponds to the timing capillary blood engorgement in the ear resulting in a reduction in infrared scatter to the PPG collector. The difference between the timings illustrated in **797** and **796** for that one cardiac cycle is the pulse transit time from the aortic valve to the in-ear sensor. The pulse-wave velocity can be calculated as the vascular distance travelled by the blood from the aortic valve to the in-ear sensor divided by the pulse-transit time. In adults that distance stays fixed and changes in pulse-transit time are inversely related to changes in pulse-wave velocity.

FIGS. **8A** and **8B** illustrate an embodiment of the glymphatic flow, brain proteinopathy and neurodegeneration tar-

get data acquisition module **800** of the system configured in accordance with the present invention and is not intended to limit scope as one of ordinary skill would understand on review of this application that other configurations could be utilized without departing from the scope of the claimed invention. Referring to FIG. **8A**, in one embodiment **810**, glymphatic flow imaging can be used with diffusion tensor MRI to measure the glymphatic flow of CSF in the perivascular spaces or can be used with a CSF tracer such as gadolinium that when injected intrathecally is cleared through the brain's extravascular, glymphatic flow, transport. Timing the injection just before the onset of sleep, an MRI scan can be done prior to sleep and once again at the end of sleep. The difference in the intensity of the contrast agent in key regions of interest provides a neuroimaging target of glymphatic system function that occurred during sleep.

In another embodiment **830**, a PET scan can be used with a radiotracer specific for a particular protein of interest and relative standard uptake value (SUVr) that quantifies the proteinopathy build up in the brain. In another embodiment, the radiotracer binds to a soluble form of the proteinopathy protein and the PET scan SUVr quantifies the change in concentration of the soluble protein following sleep.

In another embodiment, MRI **850** can be used to measure changes in brain volume, or degree of neurodegeneration, in anatomical regions of interest such as the hippocampus, entorhinal cortex, thalamus, orbitofrontal, parietal, temporal, anterior, and posterior cingulate and the precuneus regions over two time points separated by several months to provide an target rate of neurodegeneration for an individual.

In another embodiment **870**, spinal fluid concentration of a proteinopathy protein is assayed either in the morning or both before and after sleep. The absolute concentration levels normed to a population or the diurnal difference in concentration before and after sleep provide a target molecular marker for that protein that measures glymphatic flow as net clearance of the protein and also serves as a marker of brain proteinopathy and neurodegeneration.

In another embodiment **890**, plasma concentration of a proteinopathy protein is assayed either in the morning or both before and after sleep. The absolute concentration levels normed to a population or the diurnal difference in concentration before and after sleep provide a target molecular marker for that protein that measures glymphatic clearance function as net glymphatic clearance of the protein and also serves as a marker of brain proteinopathy and neurodegeneration.

The target marker data acquisition module **800** can be implemented using one of embodiment **810**, **830**, **850**, **870**, or **890**. Alternatively, the target marker data acquisition module **800** can be implemented using a plurality of the embodiments illustrated in FIG. **8** in combination.

Referring to FIG. **8B**, **812** and **814** shows a PET scan and SUVr marker for amyloid protein in two distinct individuals. Illustrated in **816** is the SUVr scale with values near 0 signifying low tracer concentrations that occurs when there is low or no amyloid proteinopathy for the tracer to bind to. Values above 1.5 indicate high tracer concentrations that occur with high amyloid build up. The PET scan illustrated in **812** shows no buildup of amyloid in any of the brain region of interest seen in this coronal slice. In contrast, the scan illustrated in **814** shows significant buildup of amyloid in many regions (indicated by arrows) of interest including orbitofrontal and temporal. Important markers of a PET scan include the SUVr value by region of interest for the protein

of interest that can be used in connection with the target prediction model. For example, the markers in the PET scans illustrated in FIG. 8B can be used as targets in training the target prediction model. Once the target prediction model is trained, new EEG features and neurovascular features can be input into the target prediction model to predict new target markers of neurodegeneration. The target marker data acquisition module 800 can be implemented using one of embodiment 810, 830, 850, 870, or 890. Alternatively, the target marker data acquisition module 800 can be implemented using a plurality of the embodiments illustrated in FIG. 8 in combination.

FIG. 9 illustrates an embodiment of the biomarker learning module 900 of the system configured in accordance with the present invention and is not intended to limit scope as one of ordinary skill would understand on review of this application that other configurations could be utilized without departing from the scope of the claimed invention. Referring to FIG. 9, in one embodiment, 901 input data can be the neurophysiology feature data acquired by module 600, neurovascular feature data acquired by module 700, or a combination thereof, and glymphatic flow target data acquired by 810 of module 800. In another embodiment, 901 input data can be a marker of glymphatic flow acquired by 810 and molecular or neuroimaging target output data acquired by module 800 can be any one of the embodiments described by 830, 850, 870 or 890 in FIG. 8A or a combination thereof. The target marker data can be continuously valued, for example a pseudo-diffusion coefficient to measure glymphatic flow in mm<sup>2</sup>/sec using diffusion tensor MRI, SUVr in a PET scan or picomolar concentrations in spinal fluid molecular assays of protein, or can be categorical valued such as high or low based on thresholding the continuous valued measures using standardized levels for a disease stage. Target neuroimaging marker data can be whole brain values or values for specific regions of interest known to be primarily affected by the specific neurodegenerative disease process. The input training data 901 needs to be carefully collected on a population of 12 or more patients at varying levels of the disease process ranging from unaffected to very affected. Having data representative of patients at different extremes of the disease process gives a range of target marker data values, for example as was shown in the amyloid PET scan SUVr values in FIG. 8B for an unaffected patient 812 and a patient with advanced amyloidosis in the brain 814. These extreme values enable the prediction model and fitting procedure 903 to learn the combination of feature patterns in the neurophysiology data 600 and neurovascular data 700 that correspond to unaffected patients and those that correspond to affected patients. Each patient data needs to be collected concurrently with neurophysiology data and neurovascular data collected together for one or more nights around the time of the target glymphatic flow, molecular or neuroimaging marker data. The device illustrated in FIG. 1 is designed to capture concurrent, time synchronized neurophysiology data and neurovascular data from a patient, and to ensure repeatability of the data acquisition by ensuring consistency of the positioning of all the sensors using the anatomically form-fitted ear device illustrated in FIG. 2G. Repeating acquisition of the neurophysiology data and neurovascular data over several nights yields additional features for training the prediction model in 903 that improves the bias-variance tradeoff of model fitting and improves predictions. The neurophysiology data and neurovascular data is preprocessed by performing feature extraction as is illustrated in FIGS. 6A-F and FIGS. 7A-E.

In 903, a model and fitting procedure are selected. The model can be one of many known machine learning and deep learning models, including those used in commercially available software packages and services, and the fitting procedure is selected based on the model selected. Random forest, a general-purpose machine learning model, works very well to identify the patterns and ranges of the neurophysiology and neurovascular feature values that best separate, or predict, the target glymphatic flow, molecular or neuroimaging markers. Acquiring the patient training data is expensive and requires an investigational review board approved clinical study. Random forest has the advantage over deep learning models in that it provides good results on a relatively small number of patient data examples. Once the model is learned on a population of patients representative of the target application, predictions of brain glymphatic flow, proteinopathy or neurodegeneration in new, unseen patients can be made from the neurophysiology and neurovascular sleep data acquired by the device illustrated in FIG. 1A without subjecting a patient to expensive and invasive clinical procedures such as brain MRI, cerebrospinal fluid molecular analysis or PET neuroimaging. This allows the device illustrated in FIG. 1A to both screen for markers of indicating out-of-range values of glymphatic flow, brain proteinopathy or neurodegeneration and to monitor progression of those markers over time for individuals that screen positive.

Once a model such as random forest is selected, the neurophysiology and neurovascular data are input features and the target marker data is the target output in the model cross validation 905. The patient data of 901 is first randomly split into a number of folds, such as five non-overlapping sets. The model in 903 is fit to the data of the first four folds and the fitted model is used to predict the target marker data of the patients in the 5<sup>th</sup> fold. This procedure is repeated four more times, each time leaving out a new fold of patients and their data, resulting in model predictions of the complete target marker data from the input neurophysiology and neurovascular feature data. In 907 the model is evaluated using a goodness-of-fit metric that can be the root-mean-square between the prediction in 903 and the target marker data. Operations 901-907 can be repeated using several different models to determine which provides the most accurate prediction of the target marker data. The best target prediction model is promoted to 909 where holdout patients and their data, including target marker data that has never been seen by the model, is tested and the prediction model and its performance on the holdout data is outputted in 911.

FIG. 10 illustrates an embodiment of the target prediction module 1000 of the system configured in accordance with the present invention and is not intended to limit scope as one of ordinary skill would understand on review of this application that other configurations could be utilized without departing from the scope of the claimed invention. Referring to FIG. 10, in one embodiment, 1001 is new neurophysiology and neurovascular data acquired by modules 600 and 700 from an individual and are inputted into the target prediction model output of 911. Features are extracted from the data as illustrated in FIG. 6A-F and FIG. 7A-E. The new neurophysiology and neurovascular data can be acquired from a new, unseen patient or from a patient that was part of the original training data but the new data is acquired several months or years later to evaluate progression of disease. In operation 1003, the module executes the target prediction model on the new input data of operation 1001 and outputs a marker of glymphatic flow 1005. In

another embodiment, **1001** is the glymphatic flow output of the target prediction model **1005** and in operation **1003**, the module executes the target prediction model on this new input data of operation **1001** and outputs a marker of brain proteinopathy or neurodegeneration **1005**.

The target prediction can be a predicted value for glymphatic flow, a level of a protein accumulation such as those described previously or a degree of neurodegeneration measured as changes in whole-brain volume or regional volume using structural MRI. The predictions can be continuous values of marker values used to monitor for disease progression or response to intervention, or categorical values to determine the presence or absence of a disease stage. The target predictions of disease stage classification can be submitted for regulatory approval with the appropriate regulatory validation study and reporting of sensitivity, specificity, positive and negative predictive values compared to a gold-standard target such as a molecular analysis or neuroimaging test.

FIG. **11A-C** illustrate an embodiment of the target engagement module **1100** of the system configured in accordance with the present invention and is not intended to limit scope as one of ordinary skill would understand on review of this application that other configurations could be utilized without departing from the scope of the claimed invention. Referring to FIG. **11A**, in one embodiment, the target engagement module **1110** records data from an intervention before sleep or during sleep, module **1130** records the neurophysiology and neurovascular data during sleep and input data from the intervention in operation **1110**. In module **1150**, engagement of the intervention with one of a neurophysiology target or feature, illustrated in FIG. **6A**, or one of a neurovascular target or feature, illustrated in FIG. **7A**, or a combination of either, is computed as the change in the neurophysiology or neurovascular feature value from baseline. The process **1110**, **1130** and **1150** can be repeated multiple times at different levels or dosing intensities of the therapeutic intervention to establish a target engagement response curve.

The prediction model **911** can be executed using data inputs **1110** and **1130** to output a prediction of the therapeutic intervention's expected impact on glymphatic flow, brain proteinopathy or neurodegeneration in the short term or if sustained in the long term. The glymphatic flow, brain proteinopathy or neurodegeneration prediction that is output can be used to show the effect of the intervention on the glymphatic flow, molecular or neuroimaging marker of neurodegeneration. In other embodiments, operation **1110** can record cardiovascular, diet, pharmaceutical or neuro-modulation interventions, which data is then input into **1130** for execution computation of target engagement at operation **1150**. As such, the effect of the interventions on the neurophysiology and neurovascular data can be ascertained and using the prediction model **911** the intervention's effect on a marker of neurodegeneration determined.

Referring to FIG. **11B**, in one embodiment an input intervention can be raising (reverse Trendelenburg) or lowering (Trendelenburg) the head relative to the feet relative to a flat supine position as illustrated in **1112**. Trendelenburg increases intracranial perfusion pressure. Monitoring the transcranial impedance in **1134** during the interventions of **1112** shows that the transcranial impedance decreased with Trendelenburg and returned to normal as the patient was returned to a flat supine position, demonstrating target engagement of this intervention with cerebral fluid volume. Monitoring the amplitude envelope of in-ear PPG tracing in **1132** shows the reverse occurring with Trendelenburg

decreasing the amplitude, or blood volume, going to the ear and scalp and returning to normal when the patient is returned to a flat supine position.

In another embodiment, an input intervention can be a cardiopulmonary intervention such as a Valsalva maneuver or hyperventilation. The transcranial impedance tracing following these two cardiopulmonary interventions are illustrated in **1136** and **1138**. In **1136** the patient performed a 45 second Valsalva maneuver starting at the 1-minute mark. The Valsalva maneuver increases intrathoracic pressure thereby decreasing venous return from the head. The decrease in venous return results in venous engorgement and increase in cerebral fluid volume. This is demonstrated by the decrease in the transcranial impedance during the Valsalva in tracing **1136**. In **1138**, the same patient started hyperventilating lightly at 1 minute and progressed to full hyperventilation at 1 minute and 15 seconds. Each inspiration decreases intrathoracic pressure and increases venous return, causing a decrease in cerebral fluid volume and an increase in transcranial impedance, as shown in tracing **1138**. In both these interventions, monitoring a neurovascular tracing demonstrated target engagement of the intervention with the neurovascular measure, in this case cerebral fluid volume.

Referring to FIG. **11C**, in another embodiment when target engagement of an intervention with one or more of the neurophysiology and neurovascular data has been determined, the prediction model **911** is used to determine the intervention's effect on a marker of glymphatic flow, brain proteinopathy or neurodegeneration. Illustration **1152** shows rates of clearance of intrathecal gadolinium from the brain measured by serial MRI under three different interventions. The first intervention is control, that is normal sleep with no intervention, the second intervention is sleep deprivation and the third intervention is dexmedetomidine that increases the duration of slow wave sleep. These three interventions engage sleep EEG measures, particularly slow wave sleep duration. Illustration **1152** shows corresponding slower clearance of the contrast agent with sleep deprivation (no slow wave sleep) compared to control, and control shows slower clearance than dexmedetomidine (increased slow wave sleep), as expected from prediction model **911** that is trained on sleep EEG data, neurovascular data and target brain proteinopathy and neurodegeneration data.

#### Embodiments Set Forth as Clauses

In addition to the forgoing, the various embodiments of the present disclosure include, but are not limited to, the embodiments set forth in the following clauses.

Clause 1. A method implemented with one or more computer processors, the method comprising:

- a. accessing, by the one or more computer processors, neurophysiological data and neurovascular data recorded during sleep;
- b. executing, by the one or more computer processors, a function mapping from said neurophysiological data and neurovascular data to a target that is a marker of glymphatic flow; and
- c. outputting, by the one or more computer processors, a target prediction model based on the function mapping.

Clause 2. The method of clause 1, further comprising:

- a. executing, by the one or more computer processors, a second function mapping from the marker of glymphatic flow to a target that is one of a molecular analysis marker of neurodegeneration or a neuroimaging marker of neurodegeneration; and

## 21

b. outputting, by the one or more computer processors, a target prediction model based on the second function mapping.

Clause 3. The method of clause 1, wherein the neurophysiological data are electroencephalogram recordings, and sleep macrostructure and sleep microstructure features are extracted from the electroencephalogram recordings.

Clause 4. The method of clause 1, wherein the neurovascular data comprise one or more of electrical impedance recordings taken from a patient's head, photoplethysmography measured at the patient's head, and inertial measurement unit acceleration measured in a patient's ear, wherein the neurovascular data are used to compute sleep cerebral fluid volume changes, cerebral perfusion pulsation, heart rate variability, resting heart rate, pulse transit time, pulse wave velocity and respiratory rate.

Clause 5. The method of clause 1, wherein the neurophysiological data and neurovascular data are acquired from a wearable device.

Clause 6. The method of clause 5, wherein sensors of the wearable device are inserted into an ear of a patient and measurements are taken from the ear or ear canal.

Clause 7. The method of clause 6, wherein the wearable device has a bladder that is pressurized inside the ear canal to increase the interfacial surface contact of the sensors to the canal a wall of the ear canal.

Clause 8. The method of clause 2, wherein the molecular analysis marker of neurodegeneration is a CSF or blood plasma assay of one of  $\beta$ -amyloid, tau, p-tau,  $\alpha$ -synuclein, and neurofilament light.

Clause 9. The method of clause 2, wherein the neuroimaging marker of neurodegeneration is a PET scan with a radiotracer that binds to one of  $\beta$ -amyloid, tau, or glucose.

Clause 10. The method of clause 2, wherein the neuroimaging marker of neurodegeneration is an MRI scan.

Clause 11. The method of clause 1, further comprising: inputting new neurophysiological data and new neurovascular data into the target prediction model; and outputting a predicted marker of glymphatic flow.

Clause 12. The method of clause 1, further comprising: inputting intervention data into the target prediction model;

inputting new neurophysiological data and new neurovascular data into the target prediction model; outputting a predicted target marker of glymphatic flow; and

determining an effect of the intervention data on the predicted target marker of glymphatic flow.

Clause 13. A system comprising:

one or more computer processors;

a neurophysiological data acquisition module configured to measure neurophysiological data;

a neurovascular data acquisition module configured to measure neurovascular data; and

a transmission module configured to transmit the electroencephalogram data and the neurovascular data to a second computing device.

Clause 14. The system of clause 13, wherein the one or more computer processors, the neurophysiological data acquisition module, the neurovascular data acquisition module, and the transmission module are disposed in a wearable device.

Clause 15. The system of clause 14, wherein the wearable device is configured to attach to an ear of a patient.

Clause 16. The system of clause 15, wherein sensors of the wearable device are inserted into the ear and measurements are taken from the ear or ear canal.

## 22

Clause 17. The system of clause 16, wherein the wearable device comprises a bladder that is pressurized inside the ear canal to increase interfacial surface contact of the sensors to a wall of the ear canal.

Clause 18. The system of clause 13, wherein the neurophysiological data are electroencephalogram recordings, and sleep macrostructure and sleep microstructure features are extracted from the electroencephalogram recordings.

Clause 19. The system of clause 13, wherein the neurovascular data comprise one or more of electrical impedance recordings taken from a patient's head, photoplethysmography measured at the patient's head, and inertial measurement unit acceleration measured in a patient's ear, wherein the neurovascular data are used to compute sleep cerebral fluid volume changes, cerebral perfusion pulsation, heart rate variability, resting heart rate, pulse transit time, pulse wave velocity and respiratory rate.

Clause 20. The system of clause 13, wherein the second computing device is one of a mobile telephone, a local computing device, and a remote computing device.

Clause 21. The system of clause 13, wherein the second computing device comprises a machine learning algorithm configured to input the neurophysiological data and the neurovascular data and configured to output a target prediction model.

Clause 22. The system of clause 21, wherein the target prediction model is configured to receive as input new neurophysiological data and new neurovascular data and configured to output a predicted marker of neurodegeneration.

Clause 23. The system of clause 21, wherein the target prediction model is configured to receive as input intervention data, new neurophysiological data, and new neurovascular data, and configured to output a predicted marker of brain proteinopathy or neurodegeneration, and a determination of an effect of the intervention data on the predicted marker of brain proteinopathy or neurodegeneration.

Clause 24. A method implemented with one or more computer processors, the method comprising:

a. accessing, by the one or more computer processors, neurophysiological data and neurovascular data recorded during sleep;

b. executing, by the one or more computer processors, a function mapping from said neurophysiological data and neurovascular data to a target, the target being one or more of a marker of glymphatic flow, a molecular analysis marker of neurodegeneration, or a neuroimaging marker of neurodegeneration;

c. outputting, by the one or more computer processors, a target prediction model based on the function mapping;

d. receiving, as an input, newly collected neurophysiological data and neurovascular data collected during sleep into the target prediction model;

e. receiving, as an input, data associated with a therapeutic intervention; and

f. measuring an effect of the therapeutic intervention.

Clause 25. A method implemented with one or more computer processors, the method comprising:

a. activating a neurophysiological data sensor and a neurovascular data sensor of a wearable device;

b. gathering, by the sensors, neurophysiological data and a neurovascular data during sleep;

c. storing the neurophysiological data and the neurovascular data in a storage device of the wearable device;

d. process the neurophysiological data and the neurovascular data using a processor of the wearable device; and

23

e. transmitting, by a transmission module of the wearable device, the neurophysiological data and the neurovascular data to a second computing device.

Clause 26. A non-transitory computer-readable medium comprising computer-executable instructions performing the operations recited in clause 1. 5

Clause 27. A non-transitory computer-readable medium comprising computer-executable instructions performing the operations recited in clause 24.

Clause 28. A non-transitory computer-readable medium comprising computer-executable instructions performing the operations recited in clause 25. 10

What is claimed:

1. A brain monitoring system comprising:

left electrodes and right electrodes that collect neurovascular measurements from a patient's head during a sleep interval; and 15

a computing module that:

receives transcranial impedance data derived from the neurovascular measurements collected by the left electrodes and right electrodes, 20

applies the transcranial impedance data to a model to determine an indication of glymphatic flow, and responsive to the indication of glymphatic flow, performs at least one of: a) displaying the indication of glymphatic flow on a display, and b) administering a therapeutic intervention. 25

2. The brain monitoring system of claim 1, wherein the computing module further receives electroencephalogram data derived from neurophysiological measurements collected by the left electrodes and the right electrodes, and wherein the model is derived from the electroencephalogram data. 30

3. The brain monitoring system of claim 1, wherein the computing module performs the administering of the therapeutic intervention and wherein the therapeutic intervention is a neuromodulation intervention. 35

4. The brain monitoring system of claim 3, wherein the computing module modifies an intensity of the neuromodulation intervention. 40

5. The brain monitoring system of claim 3, wherein the computing module further determines and displays a measure of an effect of the neuromodulation intervention.

6. The brain monitoring system of claim 1, further comprising an input device that receives instructions for the therapeutic intervention. 45

7. The brain monitoring system of claim 1, further comprising a flexible band, wherein the left electrodes and the right electrodes are coupled to the flexible band.

8. The brain monitoring system of claim 1, wherein the computing module further determines and displays an effect of a pharmaceutical intervention. 50

9. The brain monitoring system of claim 8, wherein the pharmaceutical intervention comprises a dosage of dexmedetomidine. 55

10. The brain monitoring system of claim 1, wherein an initial therapeutic intervention is administered to the patient while the neurovascular measurements are collected from the patient's head during the sleep interval.

11. A brain monitoring system comprising: 60

left electrodes and right electrodes that collect neurovascular measurements from a patient's head during a sleep interval; and

a computing module that:

receives transcranial impedance data derived from the neurovascular measurements collected from the left electrodes and the right electrodes, 65

24

applies the transcranial impedance data to a model to determine an indication of fluid flow in intracranial perivascular pathways, and

responsive to the indication of fluid flow in the intracranial perivascular pathways, performs at least one of: a) displaying the indication of fluid flow in the intracranial perivascular pathways on a display, and b) administering a therapeutic intervention.

12. The brain monitoring system of claim 11, wherein the computing module further receives electroencephalogram data derived from neurophysiological measurements collected by the left electrodes and the right electrodes, and wherein the model is derived from the electroencephalogram data.

13. The brain monitoring system of claim 11, wherein the computing module performs the administering of the therapeutic intervention and wherein the therapeutic intervention is a neuromodulation intervention.

14. The brain monitoring system of claim 13, wherein the computing module modifies an intensity of the neuromodulation intervention.

15. The brain monitoring system of claim 13, wherein the computing module further determines and displays a measure of an effect of the neuromodulation intervention.

16. The brain monitoring system of claim 11, further comprising an input device that receives instructions for the therapeutic intervention.

17. The brain monitoring system of claim 11, further comprising a flexible band, wherein the left electrodes and the right electrodes are coupled to the flexible band.

18. The brain monitoring system of claim 11, wherein the computing module further determines and displays an effect of a pharmaceutical intervention.

19. The brain monitoring system of claim 18, wherein the pharmaceutical intervention comprises a dosage of dexmedetomidine.

20. The brain monitoring system of claim 11, wherein an initial therapeutic intervention is administered to the patient while the neurovascular measurements are collected from the patient's head during the sleep interval.

21. A brain monitoring system comprising:

left electrodes and right electrodes that collect neurovascular measurements from a patient's head during a sleep interval; and

a computing module that:

receives transcranial impedance data derived from the neurovascular measurements collected from the left electrodes and the right electrodes,

applies the transcranial impedance data to a model to determine a characteristic of intracranial perivascular pathways, and

responsive to the characteristic of the intracranial perivascular pathways, performs at least one of: a) displaying the characteristic of the intracranial perivascular pathways on a display, and b) administering a therapeutic intervention. 50

22. The brain monitoring system of claim 21, wherein the computing module further receives electroencephalogram data derived from neurophysiological measurements collected by the left electrodes and the right electrodes, and wherein the model is derived from the electroencephalogram data.

23. The brain monitoring system of claim 21, wherein the computing module performs the administering of the therapeutic intervention and wherein the therapeutic intervention is a neuromodulation intervention.

24. The brain monitoring system of claim 23, wherein the computing module modifies an intensity of the neuromodulation intervention.

25. The brain monitoring system of claim 23, wherein the computing module further determines and displays a mea- 5  
sure of an effect of the neuromodulation intervention.

26. The brain monitoring system of claim 21, further comprising an input device that receives instructions for the therapeutic intervention.

27. The brain monitoring system of claim 21, further 10  
comprising a flexible band, wherein the left electrodes and the right electrodes are coupled to the flexible band.

28. The brain monitoring system of claim 21, wherein the computing module further determines and displays an effect 15  
of a pharmaceutical intervention.

29. The brain monitoring system of claim 28, wherein the pharmaceutical intervention comprises a dosage of dexmedetomidine.

30. The brain monitoring system of claim 21, wherein an initial therapeutic intervention is administered to the patient 20  
while the neurovascular measurements are collected from the patient's head during the sleep interval.

\* \* \* \* \*